The Geology of North America
Decade Map Volume 1
1991

Chapter 10

The seismicity of Nevada and some adjacent parts of the Great Basin

A. M. Rogers and S. C. Harmsen
U.S. Geological Survey, Box 25046, Denver Federal Center, Denver, Colorado 80225
Edward J. Corbett, K. Priestley, and Diane dePolo
Seismological Laboratory, University of Nevada, Reno, Nevada 89557

INTRODUCTION

The seismicity of Nevada is distributed in several broad zones that connect with significant seismic zones in surrounding states and appear to concentrate the largest earthquakes in the Great Basin province. During the historic record, which extends over the last 140 years, a number of large, damaging earthquakes occurred in some of these zones, and those larger than magnitude 6 typically produced surface rupture. Based on geologic evidence, most of these earthquakes are believed to have occurred on steeply dipping range-front normal faults that penetrate the crust to midcrustal depths. For numerous cases, however, seismic and geodetic data suggest that strike slip and oblique slip occurred at focal depths. Microearthquake data also indicate a preference for dextral strike slip and oblique slip on northerly trending, steeply dipping faults at depths ranging from near-surface to about 15 km. In addition, some discrepancy exists between the orientation of faults inferred from seismic and geologic data. Faults show a tendency to be rotated clockwise relative to preferred nodal plane orientation. Little seismic evidence has been found for slip on low-angle detachment or listric faults in spite of abundant geologic evidence for this deformation style in the last 15 m.y.

The existence of seismic evidence for transcurrent slip on northerly trending faults is at variance with popular tectonic models for the large, young structures in the region—the basins and ranges. The seismic data are also not in accord with the abundant northwest and northeast conjugate strike-slip faults that exist in the Walker Lane belt and the margins of the southern Great Basin. The tectonic framework of the seismicity of the region is, thus, incompletely understood. Discerning between various tectonic driving mechanisms could help resolve these problems. For instance, previous discussions have raised questions regarding whether Great Basin deformation is causally related to tectonics along the continental plate margin (i.e., Slemmons, 1967; Atwater, 1970), or to processes internal to the Great Basin such as an over-thickened crust (Coney and Harms, 1984), gravitational spreading (Wernicke, 1981), or other processes related to back-arc extension (Matthews and Anderson, 1973; Coney, 1987). This summary of historical and current seismicity data of the region provides a basis for evaluating contemporary deformation in terms of generalized tectonic models of the Great Basin.

SEISMICITY OVERVIEW

The seismic patterns in Nevada (Fig. 1, 2, and 3) can be discussed in terms of several significant trends. The most prominent seismic trend is the zone of moderate-to-large earthquakes extending northward from southern California into west-central Nevada. This zone was referred to as the 118°W Meridian Zone by Slemmons and others (1965) and as the Ventura-Winnemucca zone by Ryall and others (1966). The part of the zone within Nevada has been referred to as the central Nevada seismic belt (CNSB) by Wallace (1984a). We use the latter term in this chapter. This zone includes the largest Nevada earthquakes in historic time. Since 1900, three earthquakes greater than magnitude 7.0 occurred, and seven earthquakes produced surface rupture (Tables 1 and 2; magnitudes in this chapter are M_L or M_S, unless otherwise noted).

The second zone of prominent seismicity is the Sierra Nevada–Great Basin boundary zone (SNGBZ), described by Van Wormer and Ryall (1980). The zone extends northwest near the California-Nevada border from Bishop to Reno and continues for hundreds of kilometers into northern California. Earthquakes in the zone tend to concentrate along the east flank of the Sierra Nevada. In addition to frequent moderate earthquakes, large events have also occurred in 1852, 1860, and 1872. The Mammoth earthquake series is also in this zone. Five earthquakes in the SNGBZ have produced surface rupture.

The third trend that is apparent in Figure 2 is the arcuate earthquake zone extending from the south end of the Wasatch front in Utah into and across southern Nevada to eastern California near Bishop. This earthquake trend has been referred to as the

Rogers, A. M., Harmsen, S. C., Corbett, E. J., Priestley, K., and dePolo, D., 1991, The seismicity of Nevada and some adjacent parts of the Great Basin, *in* Slemmons, D. B., Engdahl, E. R., Zoback, M. D., and Blackwell, D. D., eds., Neotectonics of North America: Boulder, Colorado, Geological Society of America, Decade Map Volume 1.

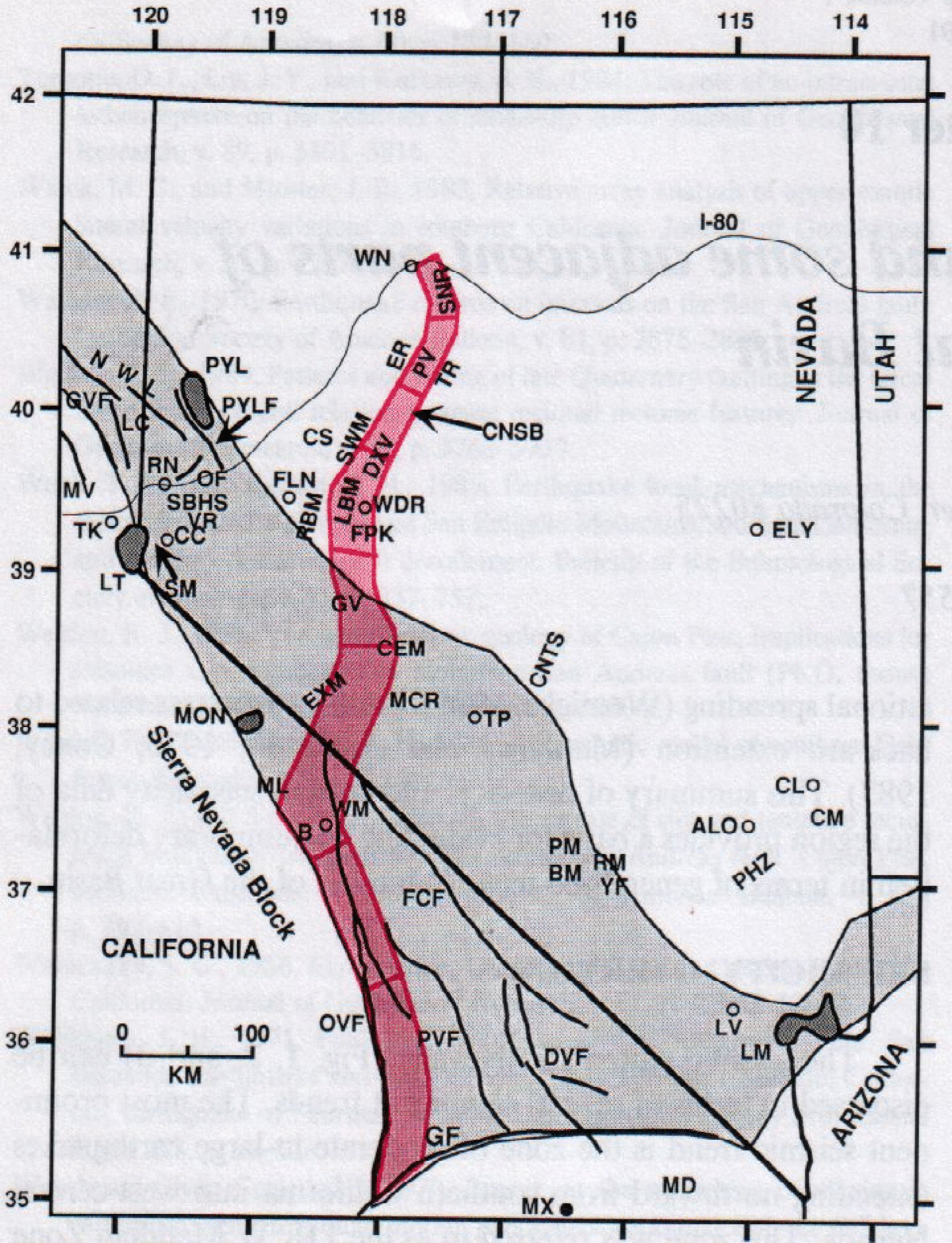

Figure 1. Map showing the location of towns, ranges, and other geographic and geologic features discussed in the text. The northwest-trending shaded zone is the Walker Lane belt as defined by Stewart (1988). The northerly trending shaded zones make up the Central Nevada Seismic Belt (CNSB) defined by Wallace (1984a). The northern most gap is the Sonoma Range gap (Thenhaus and Barnhard (1989). Breaks in the CNSB roughly denote the extent of seismic zones, fault segmentation, and gaps defined by Wallace (1984a). Other symbols are: ALO-Alamo; B-Bishop; BM-Buckboard Mesa; CC-Carson City; CEM-Cedar Mountain; CL-Caliente; CM-Clover Mountains; CNTS-Central Nevada Test Area; CS-Carson Sink; DXV-Dixie Valley; DVF-Death Valley fault; ER-East Range; EXM-Excelsior Mountain; FCF-Furnace Creek fault; FLN-Fallon; FPK-Fairview Peak; GF-Garlock fault; GV-Gabbs Valley; GV-Grizzly Valley fault; LC-Last Chance fault; LM-Lake Mead; LM-Louderback Mountains; LT-Lake Tahoe; LV-Las Vegas; MCR-Monte Cristo Range; MD-Mojave Desert; ML-Mammoth Lakes; MON-Mono Lake; MV-Mohawk Valley fault; MX-Manix earthquake; NWL-northern Walker Lane belt; OF-Olinghouse fault; OVF-Owens Valley fault; PHZ-Pahranagat Shear Zone; PM-Pahute Mesa; PV-Pleasant Valley; PVF-Panamint Valley fault; PYL-Pyramid Lake; PYLF-Pyramid Lake fault zone; RBM-Rainbow Mountain; RM-Rainier Mesa; RN-Reno; SBHS-Steamboat Hot Springs; SM-Slide Mountain; SNR-Sonoma Range; SWM-Stillwater Range; TK-Truckee; TP-Tonopah; TR-Tobin Range; VR-Virginia Range; WDR-Wonder; WM-White Mountains; WN-Winnemucca; YF-Yucca Flat.

southern Nevada Transverse Zone (NTZ) by Slemmons and others (1965) and as the east-west seismic belt by Smith (1978). The most recent maps of this area show that the NTZ may have considerable north-south expression; a north-northeasterly trending prong of activity extends from about 37.5°N and 116°W to as much as 40°N. Only small to moderate historic earthquakes have occurred in this zone, including four events of about magnitude 6 (1908 and 1916 in Death Valley, California; 1902 Pine Valley, Utah; 1966 Clover Mountains, Nevada). A fifth event, the magnitude 6.4 1947 Manix earthquake, occurred on what might be described as the southern fringe of the NTZ and produced surface rupture (Richter, 1958). Several areas of induced seismicity have affected the record in this region (see below) due to underground nuclear testing and the impoundment of Lake Mead. Excluding the Manix earthquake, the only known historic surface rupture in this zone accompanied a number of the larger underground nuclear tests. The zone might not appear to be continuous from east to west across southern Nevada if earthquakes had not been induced. A few earthquakes, however, exist in the historic record of the southern Great Basin area before underground testing or the impoundment of the lake (Meremonte and Rogers, 1987). In addition, data from regional network studies show that microearthquakes are widespread across the southern Nevada region, and many are likely unrelated to nuclear testing (Rogers and others, 1987).

All three of these trends appear to converge in the Mammoth-Bishop area, but the significance of this fact is not understood. A high percentage of Nevada earthquakes occur within these three trends, including all earthquakes over magnitude 6. Elsewhere, scattered diffuse seismicity covers the rest of Nevada at a level that is low compared to California, but high compared to other surrounding states. The apparent drop-off in seismicity at several of Nevada's borders may, however, be an artifact of a lower level of seismic monitoring in Oregon, Idaho, Utah, and Arizona.

Possible secodary seismic zones are also apparent in Figure 2. For instance, there may be one or more additional zones of seismicity that subparallel the CNSB, both on the northwest and southeast of the CNSB.

BRIEF HISTORY OF THE EARTHQUAKE RECORD IN THE GREAT BASIN

The early seismic history of the region is contained in a "Catalog of Nevada Earthquakes, 1852–1960" by Slemmons and others (1965), which they based on Indian traditions, newspaper accounts, and other historical records, as well as catalogs published by other institutions. Information on Great Basin earthquakes prior to 1916 derives mainly from catalogs developed by Holden (1898), McAdie (1907), and Townley and Allen (1939). Additional accounts of northern Nevada seismicity are given by Ryall and Douglas (1974), Ryall and Priestley (1975), and Ryall and Vetter (1982). The accuracy of pre-instrumental event locations is highly variable because the records depend on felt reports

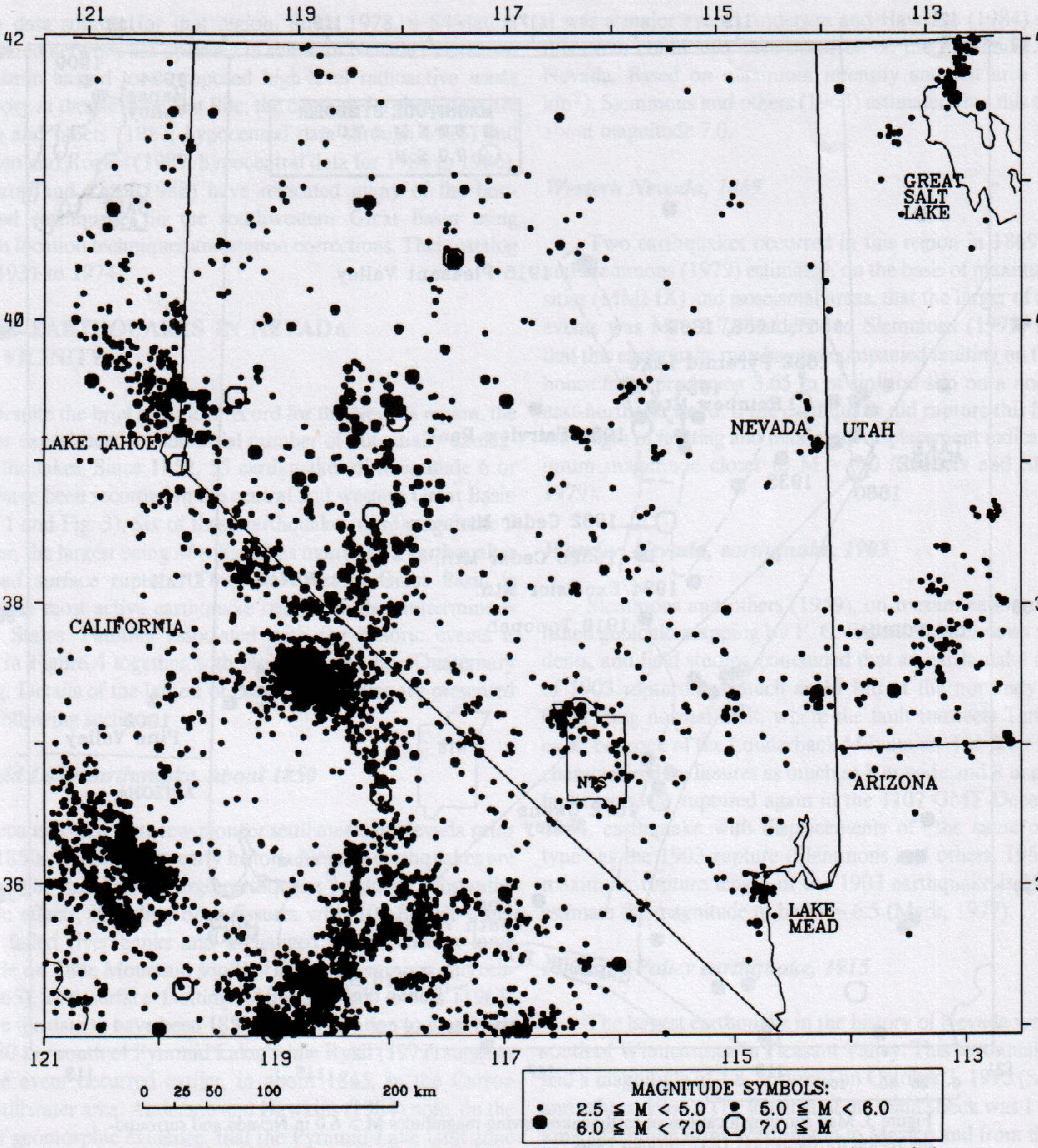

Figure 2. Map of M ≥2.5 earthquake epicenters in Nevada and surrounding areas for the time period 1850 to 1986, from Engdahl (this volume). Symbol sizes correspond to magnitudes, with smallest symbols for earthquakes having magnitudes in the range 2.5 ≤M < 4.0.

in sparsely populated Nevada, involving potential inaccuracies of several hundred km, except in cases where fault rupture was found.

The history of instrumental seismological recording in the Great Basin dates back to 1888 with the installation of a seismograph at Carson City, and 1914 with the installation of a seismograph in Salt Lake City at the University of Utah. Another station was installed in 1916 in Reno at the University of Nevada. The University of Nevada operated, semicontinuously, a two-component, horizontal Wiechert seismograph with smoked-paper recording from 1916 to 1959 (Jones, 1963, 1975). The University of California operated a three-component Sprengnether instrument on the Reno campus from 1948 until operation was taken over by the University of Nevada in 1963. Since that time, the permanent network has expanded gradually from three stations in 1962 to 74 short-period telemetered stations in 1986. With the initiation, expansion, and improvement of instrumental recording, the accuracy of earthquake locations and magnitudes

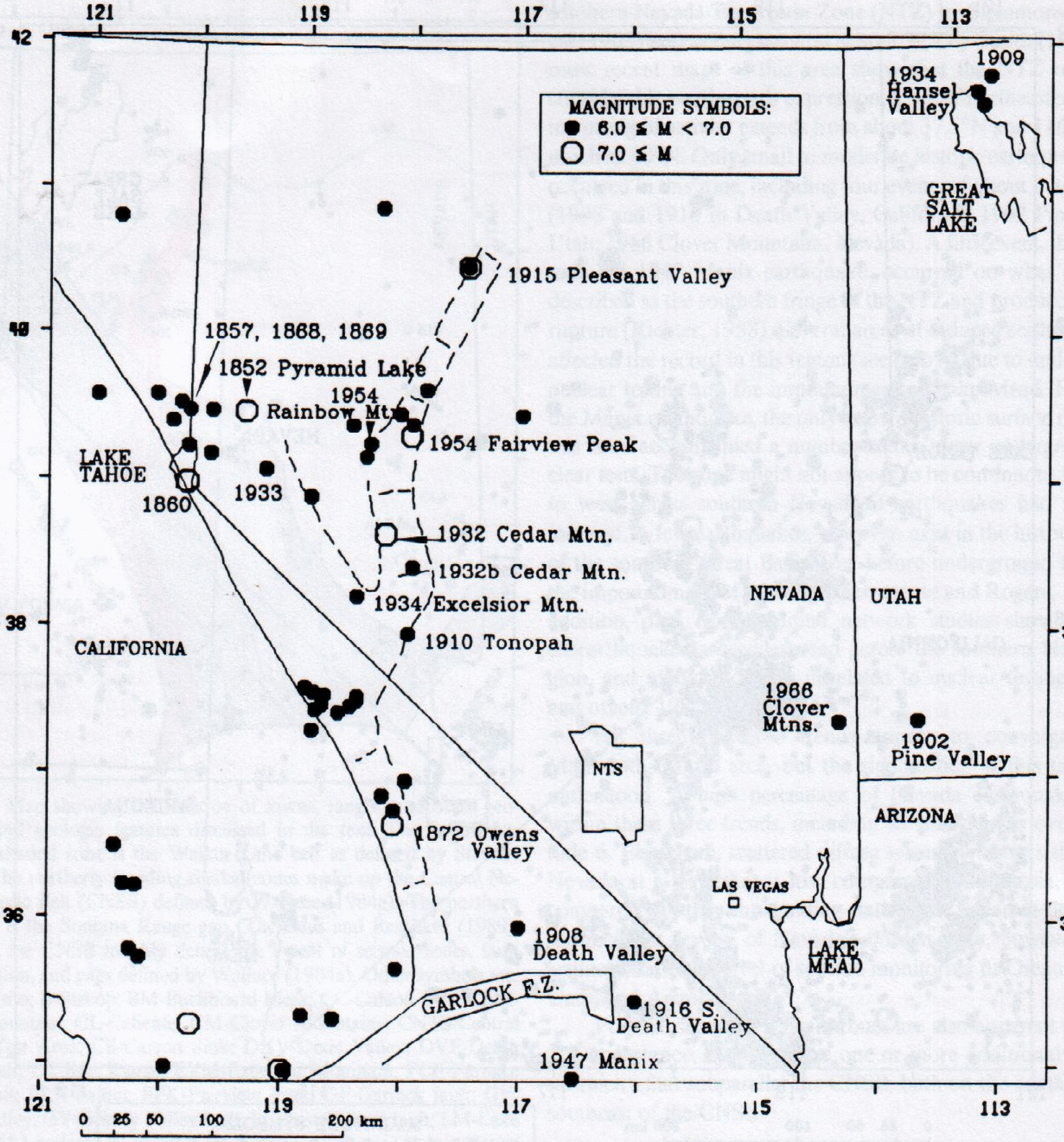

Figure 3. Map showing locations of earthquakes having magnitudes M ⩾ 6.0 in Nevada and surrounding region for the period 1852 through 1986.

increased with time. Post-1916 distance and magnitude measurements were available from the Reno Wiechert station, and combined with data from Salt Lake City, Berkeley, and later Pasadena (post-1932), location accuracies improved to within a few tens of kilometers. With the installation of modern telemetered networks in the 1970s, this accuracy improved even more. The onset of digital recording in 1981 for southern Nevada and in 1984 for northern Nevada resulted in timing accuracy of a few hundredths of a second; present-day epicenters are now accurate to less than a kilometer for the best-recorded earthquakes occurring within the denser parts of the networks. The University of Nevada Seismological Laboratory has produced annual catalogs for the northern Nevada region since 1971.

Numerous networks have operated intermittently in southern Nevada. These networks were primarily deployed to study underground-nuclear-explosion aftershocks, their associated ground motions, and earthquakes induced by the filling of Lake Mead. Because these studies were conducted by several different agencies and organizations, no complete catalog of the data exists. Meremonte and Rogers (1987) collected all known earthquake hypocenter data through 1978 for southern Nevada in a comprehensive catalog, and their report serves as a reference to all known data sources for that region. Since 1978, a 54-station telemetered network has operated in southern Nevada to evaluate the seismic hazard to a proposed high-level radioactive waste repository at the Nevada Test Site; the catalogs for these data are Rogers and others (1987; hypocentral data through 1983) and Harmsen and Rogers (1987; hypocentral data for 1984 to 1986). Gawthrop and Carr (1988) have relocated many of the best-recorded earthquakes in the southwestern Great Basin using modern location techniques and station corrections. Their catalog spans 1931 to 1974.

LARGE EARTHQUAKES IN NEVADA AND VICINITY

Despite the brief historical record for the Nevada region, the area has experienced a substantial number of potentially damaging earthquakes. Since 1852, 55 earthquakes of magnitude 6 or larger have been recorded in the central and western Great Basin (Table 1 and Fig. 3). Six of these earthquakes were magnitude 7 or larger, the largest being $M \approx 8$, and as many as 12 earthquakes produced surface rupture. Thus, the western Great Basin is among the most active earthquake regions in the conterminous United States. Faulting associated with the historic events is shown in Figure 4 together with Holocene and late Quaternary faulting. Details of the largest of these earthquakes are presented in the following sections.

Pyramid Lake earthquake, about 1850

Because there were few pioneer settlements in Nevada prior to the 1850s, details of the early historic Nevada earthquakes are sketchy. The first known large earthquake produced substantial geologic effects, including open fissures with 100-ft-high water spouts, failed river banks and a changed river course, a large landslide on Slide Mountain south of Reno (Slemmons and others, 1965), and surface faulting. Slemmons and others (1965) estimate the date to have been 1852 and the location to have been about 30 km south of Pyramid Lake, while Ryall (1977) suggests that the event occurred earlier, in about 1845, in the Carson Sink–Stillwater area. Anderson and Hawkins (1984) note, on the basis of geomorphic evidence, that the Pyramid Lake fault zone may have been the source of this earthquake. This fault demonstrates evidence of recurrent Holocene dextral strike slip on a northwest-trending fault (Table 2). The dramatic earthquake effects (maximum Modified Mercalli intensity, $MMI \approx X$) and their widespread occurrence suggest that this event was at least magnitude 7.3 (Slemmons and others, 1965).

Western Nevada, 1860

A large earthquake on March 15, 1860, was felt from California to Utah and was very violent in Carson City. Its epicenter is unknown, but a Nevada location is likely, and its wide felt area (maximum MMI IX, Slemmons and others, 1965) indicates that it was a major event. Anderson and Hawkins (1984) suggested this event could also have occurred on the Pyramid Lake fault, Nevada. Based on maximum intensity and felt area (518,000 km^2), Slemmons and others (1965) estimated that this event was about magnitude 7.0.

Western Nevada, 1869

Two earthquakes occurred in this region in 1869. Sanders and Slemmons (1979) estimated, on the basis of maximum intensities (MMI IX) and isoseismal areas, that the larger of these two events was M = 6.7. Sanders and Slemmons (1979) suggested that this earthquake may have accompanied faulting on the Olinghouse fault, producing 3.65 m of sinistral slip on a northeast to east-northeast trend. If the earthquake did rupture this fault, then the length of faulting and maximum displacement indicate a maximum magnitude closer to M = 7.0 (Sanders and Slemmons, 1979).

Wonder, Nevada, earthquake, 1903

Slemmons and others (1959), on reexamination of unpublished geologic mapping by F. C. Schrader, interviews with residents, and field studies, concluded that an earthquake in the fall of 1903 ruptured as much as 19 km of the northerly trending Gold King normal fault, where the fault transects Tertiary volcanic bedrock of the Louderback Mountains. The fault trace was characterized by fissures as much as 8 m wide and 8 m deep. The fault zone was ruptured again in the 1107 GMT December 16, 1954, earthquake with displacements of "the same order and type" as the 1903 rupture (Slemmons and others, 1959). If the maximum rupture length of the 1903 earthquake is 19 km, we estimate the magnitude to be M ≈ 6.5 (Mark, 1977).

Pleasant Valley earthquake, 1915

The largest earthquake in the history of Nevada was located south of Winnemucca in Pleasant Valley. This earthquake, which had a magnitude of 7.8, occurred on October 3, 1915 (Slemmons and others, 1965). The felt area of the main shock was 1.3 million km^2, extending from Washington to Mexico and from the Pacific to Colorado, Montana, and Arizona. The maximum intensity of this event is estimated to be MMI X. Most of the damage was to adobe or stone buildings at the mining town of Kennedy and the few ranches in the epicentral region (Jones, 1915; Page, 1935). Based on newspaper reports, Ryall and Priestley (1975) and Ryall and Vetter (1982) infer that this earthquake was preceded by moderate seismicity for several decades prior to the main shock. Six or seven events of magnitude 4 to 4.5 occurred between 1872 and 1900, no events from 1901 to 1914, and two events immediately preceded the main shock in 1915. The largest of these foreshocks, M = 6.3 (maximum MMI VIII), occurred on the day of the main shock. The main shock was also followed by an intense aftershock series (Jones, 1915).

TABLE 1. EARTHQUAKES IN NEVADA AND VICINITY MAGNITUDE ≥6; 1852 THROUGH 1986

Date yr	mo	day	Time UT	Latitude °N	Longitude °W	Max. mag.	Region
1852				39.5	119.5	7.3*	Pyramid Lake, Nevada
1857	9	3	0305	39.5	120.0	6.2	Southwest of Reno; Nevada-California border
1860	3	15	1845	39.	120.	7.0*	West Carson City, Nevada
1868	5	30	0511	39.25	120.	6.0	West Carson City, Navada
1868	9	4	1600	37.	118.	6.3	Owens Valley, California
1869	12	27	0135	39.5	120.	6.7*	Virginia City, Nevada
1869	12	27	0940	39.5	120.	6.1	Virginia City, Nevada
1872	3	26	1030	36.7	118.1	8.0*	Lone Pine, Owens Valley, California
1872	3	26	1406	36.9	118.2	6.7	Lone Pine, Owens Valley, California
1872	4	3	1215	36.9	118.2	6.6	Lone Pine, Owens Valley, California
1872	4	11	1900	37.5	118.5	6.9	Lone Pine, Owens Valley, California
1872	11	12		39.5	117.	6.0	Austin, Nevada
1875	1	24	1200	39.6	120.3	6.0	Reno, Nevada
1887	6	3	1048	39.2	119.8	6.3	Carson City, Nevada
1896	8	17	1130	36.8	118.1	6.4	Owens Valley, California
1902	11	17	1950	37.393	113.520	6.3	Pine Valley, Utah
1903				39.5	118.1	6.5*	Wonder, Nevada
1908	11	4	0837	36.0	117.0	6.5	Death Valley, California
1909	10	6	0250	41.766	112.666	6.3	Hansel Valley, Utah
1910	11	21	2323	38.	118.	6.3	Tonopah, Nevada
1914	2	18	1817	39.5	119.8	6.0	Reno, Nevada
1914	4	24	0834	39.5	119.8	6.4	Reno, Nevada
1915	10	3	0149	40.5	117.5	6.1	Pleasant Valley, Nevada
1915	10	3	0653	40.5	117.5	7.8*	Pleasant Valley, Nevada
1916	11	10	0911	35.5	116.	6.1	Southern Death Valley?, California
1918	3	12	1030	39.580	120.830	6.3	Reno, Nevada
1927	9	18	0207	37.500	118.750	6.0	Bishop, California
1932	12	21	0610a	38.68	118.21	7.2*	Cedar Mountain, Nevada
1932	12	21	0610b	38.46	117.97	6.2*	Cedar Mountain, Nevada
1933	6	25	2045	39.1	119.3	6.0	Wabuska/Yerington, Nevada
1934	1	30	2016	38.26	118.46	6.3*	Excelsior Mountain, Nevada
1934	12	3	1505	41.658	112.795	6.6	Hansel Valley, Utah
1934	12	3	1820	41.571	112.745	6.1	Hansel Valley, Utah
1941	8	30	1328	40.900	118.300	6.0	Winnemucca, Nevada
1941	9	14	1643	37.570	118.730	6.0	Mammoth Lakes, California
1941	14	14	1839	37.570	118.730	6.0	Mammoth Lakes, California
1942	5	28	0039	40.800	120.700	6.0	Northern Walker Lane, California
1946	3	15	1349	35.716	118.050	6.3	Owens Valley, California
1948	12	29	1253	39.55	120.08	6.0	Verdi, California
1954	7	6	1113	39.29	118.36	6.8*	Fallon/Rainbow Mountain/Stillwater Range, Nevada
1954	7	6	2207	39.20	118.40	6.4	Fallon/Rainbow Mountain/Stillwater Range, Nevada
1954	8	24	0551	39.35	118.34	6.8*	Fallon/Rainbow Mountain/Stillwater Range, Nevada
1954	12	16	1107	39.20	118.00	7.3*	Fairview Peak, Nevada
1954	12	16	1111	39.67	117.87	6.9*	Dixie Valley/Stillwater Range, Nevada
1959	3	23	0710	39.43	117.99	6.3	Dixie Valley/Stillwater Range, Nevada
1959	6	23	1435	38.92	118.89	6.3	Southwest Fallon, Nevada
1966	8	16	1802	37.395	114.206	6.0	Caliente/Clover Mountains, Nevada
1966	9	12	1641	39.420	120.150	6.0	North Truckee, Nevada
1980	5	25	1633	37.589	118.826	6.5	Mammoth Lake, California
1980	5	25	1649	37.620	118.900	6.0	Mammoth Lake, California
1980	5	25	1944	37.331	118.830	6.7	35 km west-southwest Bishop, California
1980	5	27	1451	37.470	118.802	6.3	South Mammoth Lake, California
1984	11	23	1808	37.456	118.602	6.2	Round Valley, west-northwest Bishop, California
1986	7	20	1429	37.540	118.439	6.2	Chalfant Valley, Bishop, California
1986	7	21	1442	37.540	118.442	6.6*	Chalfant Valley, Bishop, California

Note: An asterisk (*) in the magnitude column refers to a surface-rupturing event. Max. mag. indicates maximum reported M_L or M_S magnitude.

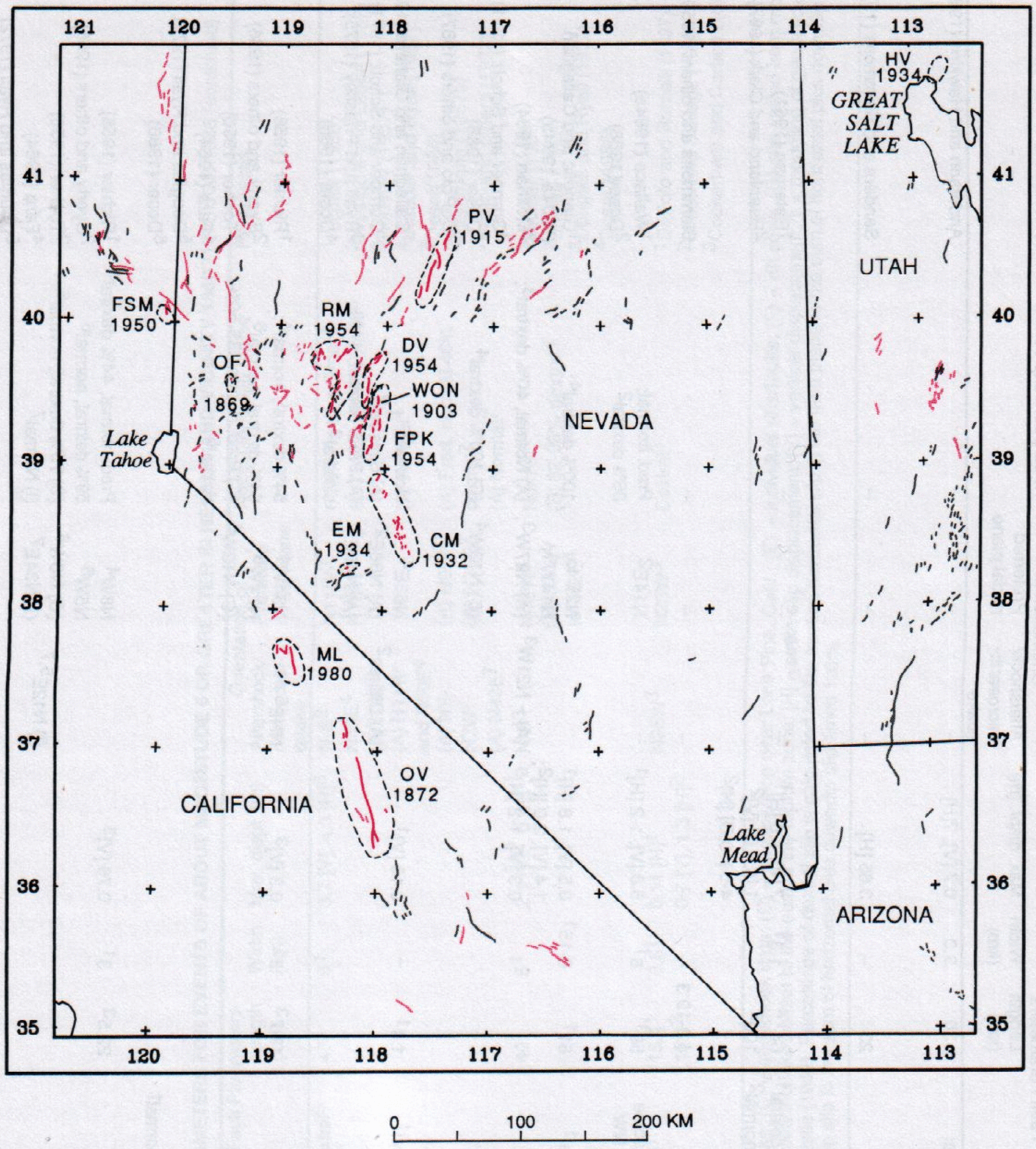

Figure 4. Map of historic (red), Holocene (shaded red), and late Quaternary (gray) faulting in Nevada and vicinity. Faulting has been adopted from Nakata and others (1982) by Thenhaus and Barnard (1989). Symbols are: CM-Cedar Mountain; DV-Dixie Valley; EM-Excelsior Mountain; FPK-Fairview Peak; FSM-Fort Sage Mountain; HV-Hansel Valley; ML-Mammoth Lakes; OV-Owens Valley; OF-Olinghouse; PV-Pleasant Valley; RM-Rainbow Mountain; WON-Wonder.

Scarps were formed along the west base of four mountain blocks in this earthquake, in some places forming new scarps and in other places breaking existing scarps (Wallace, 1984b). These blocks compose parts of the Tobin and Stillwater Ranges. The scarps formed along a zone 6 km wide and 59 km long, trending N25°E. The maximum vertical displacement on these faults is 5.8 m. Wallace (1984b) found evidence for 1 to 2 m of right slip in several locations. In a waveform modeling study, Doser (1988) found this event to be composed of two subevents that occurred on a fault striking N14°E with predominantly dip slip and some dextral slip.

Cedar Mountains earthquake, 1932

This earthquake, which occurred in the Monte Cristo Valley, west of Cedar Mountain on December 21, 1932, was M = 7.2 (Slemmons and others, 1965) and was felt over an area of 1.6 million km^2 (Coffman and von Hake, 1973). The earthquake was accompanied by about 61 km of discontinuous rifts in a belt 6 km to 15 km wide trending N21°W (Gianella and Callaghan, 1934a, 1934b). Horizontal displacements as great as 0.9 to 1.8 m and maximum vertical components of 0.5 m were measured (Gianella and Callaghan, 1934a, 1934b). The rifted zones dis-

TABLE 2. SEISMIC AND GEOLOGIC SOURCE PARAMETERS FOR EVENTS OF ABOUT MAGNITUDE 6 OR GREATER IN NEVADA AND VICINITY 1860 THROUGH 1986

Year	Region/place name	Fault Parameters: Orientation	Fault Parameters: Slip Sense	Fault Parameters: Length (km)	Fault Parameters: Width (km)	Fault Parameters: Max. displ. (m)	Orientation of: Aftershock/microearthquake	Orientation of: Preferred nodal plane	Nodal plane slip sense	References
1860	Pyramid Lake, Nevada (Pyramid Fault?)	N30W	Dextral, normal	~30	3.0	0.7 [V], ?[H]	--	--	--	Anderson and Hawkins (1984)
1869	S. of Pyramid Lake, Nevada (Olinghouse Fault)	N65E	Sinistral	23	--	3.65 [H]	--	--	--	Sanders and Slemmons (1970)
1872	Owens Valley, California	N20W[1]	Pred. normal, dextral[1]; pred. dextral, normal[2]	64[1]; 100[2]	1.3[1]	7 [V], 4.6 [H][1]; 1 [4.4,D] [V][2], 4-5 [10,D] [H][2]	--	--	--	[1]Bateman (1961) [2]Beanland and Clark (1987)
1903	Wonder, Nevada	N-S	Normal	4.8-19.3	--	--	--	--	--	Slemmons and others (1959)
1915	Pleasant Valley, Nevada	N25E[1]	Pred. normal, some dextral slip on NW faults[1]	59[1]	6[1]	5.8 [V], 1-2 [H][1]	--	N14E[2]	Pred. normal; 36% dextral[2]	[1]Wallace (1984a) [2]Doser(1988)
1932	Cedar Mountain, Nevada	(E) N11E, N61E, N11W[1] (F) N21W[1]	Dextral, normal[1]	61[1]	6-15[1]	0.5 [V], 1.8 [H][1] 1.4 [V], 2.0 [H][2]; 0.3 [V], 1-2 [H][5]	(A) ~ N21W[3]	N2E to N14W[4]; (A) N27W[3]; (C) N13W[4]	100% dextral[4]; (A) Normal, 40% dextral[3]; (C) 100% dextral[4]	[1]Gianella and Callaghan (1934a,1934b) [2]Molinari (1984) [3]Gumper and Scholz (1971) [4]Doser (1988) [5]DePolo and others (1987)
1934	Excelsior Mountain, Nevada	N65E[1]	Normal, sinistral[1]	1.4[1]	--	0.13 [V][1]	(A) Diffuse[2]	N68E[4] (A) N86E[2] (A) N49E[3]	Normal[4]; (A) Sinistral[2]; (A) Pred. normal, 44% sinistral[3]	[1]Callaghan and Gianella (1935) [2]Gumper and Scholz (1971) [3]Ryall and Priestley (1975) [4]Doser (1988)
07/06/54, 1113 UT; 2207 UT	Rainbow Mountain, Nevada	N15E[3] N7E†	Normal[2] 10% dextral, normal†	17.7[3]	3[1]	0.3 [V][3]	NNE[5]	N34W[4]; N24W[6]; (C) N12W[6]	54% dextral, normal[4]; 54% dextral, normal[6], (C) Pred. normal, 35-50% dextral[6]	[1]Richter (1958) [2]Byerly and others (1956) [3]Tocher (1956) [4]Fara (1964) [5]Douglas and Ryall (1972) [6]Doser (1986)
08/24/54, 0551 UT	Rainbow Mountain, Nevada	N20E[3]	Normal[2]	22.5[3]	3[1]	0.76 [V][3]	(I) N12E[5,7]	N8W[4]; N5W[6] (C) N0W[6] (I) N34E[7]	Pred. normal, 44% dextral[4] 59% dextral, normal[6] (C) 75% dextral, normal[6] (I) Normal[7]	[1]Richter (1958) [2]Byerly and others (1956) [3]Tocher (1956) [4]Fara (1964) [5]Douglas and Ryall (1972) [6]Doser (1986) [7]Ryall and Malone (1971)

TABLE 2. SEISMIC AND GEOLOGIC SOURCE PARAMETERS FOR EVENTS OF ABOUT MAGNITUDE 6 OR GREATER IN NEVADA AND VICINITY 1860 THROUGH 1986 (continued)

Year	Region/place name	Fault Parameters					Orientation of		Nodal plane slip sense	References
		Orientation	Slip Sense	Length (km)	Width (km)	Max. displ. (m)	Aftershock/ microearth-quake	Preferred nodal plane		
12/16/54 1107 UT	Fairview Peak, Nevada	N10E[1]	(G) Normal, dextral[6]	49[1]	6[1]	3.7 [V], 4.3 [H][6]	N-S[2]	N11W[3]	63% dextral, normal[3]	[1]Richter (1958)
							N50E[4]	N10W[5]	63-73% dextral, normal[5]	[2]Westphal and Lange (1967)
							(A) NNE[2]			[3]Romney (1957)
							(A) N11W and N50E[4]		(A) Normal[4]	[4]Stauder and Ryall (1967)
										[5]Doser(1986)
		N9E to N13W†	33-61% dextral, normal†				(A) NS-N7W[7]	(A) N9W[7]	(A) Pred. normal 46% dextral[7]	[6]Slemmons (1957b)
							(A) N40E[7]	(A) N36E[7]	(A) Normal[7]	[7]Smith and others (1972)
12/16/54 1111 UT	Dixie Valley, Nevada	N17E[1]	Normal[1]	40[1]	5[1]	2.1 [V][2], 0 [H][1]	N-S[3]	N10W[4]	Normal[4]	[1]Richter (1958)
								(B) N12W to N2E[4]	(B) 82-96% dextral[4]	[2]Shawe (1965)
		N2E to N6E†								[3]Douglas and Ryall (1972)
										[4]Doser (1986)
1986	Chalfant Valley, California	N11W[1]	Dextral, normal[1]	15.5[1]	0.5[1]	0.11 [H][1]	N25W[3]	N25W[3]	Dextral[3]	[1]DePolo and Ramelli (1987)
				15.0[2]		0.7 [V], 1.3 [H][2]				[2]Gross and Savage (1987)
										[3]Cockerham and Corbett (1987)

(A) = Microearthquake data; (B) = 1959 Dixie Valley earthquake; (C) = aftershock data; (D) = one location near Lone Pine, Calif.; (E) = individual rifts/faults; (F) = rift zone; (G) slip varied from mostly strike slip on the south to mostly normal on the north; (I) = microearthquakes offset to the east of the rupture zone; [H] = strike-slip displacement; [V] = vertical displacement; † = modeling of geodetic data (Whitten, 1957) by Snay and others (1985) and Savage and Hastie (1969). Percentage of dextral slip is calculated as the fraction horizontal slip in the fault plane to the sum of horizontal plus downdip slip times 100%. Percentage of normal slip is the fraction of downdip slip to the sum of horizontal plus downdip slip times 100%.

played variable orientation (Table 2), but are predominantly oriented east of north, whereas the nodal plane orientations strike north to west of north. Gianella and Callaghan (1934b) found the rifting patterns and slip style to be consistent with the southward shift of the Paradise Range–Cedar Mountain block to the south relative to the Gabbs Valley–Pilot Mountains block. Based on wave-form inversion, Doser (1988) considers the main shock to be two strike-slip events of magnitude 6.7 and 6.6, respectively, occurring about 20 seconds apart. The surface breaks occurred within a larger fault zone, termed the Stewart and Monte Cristo fault zone (SMCFZ) by Molinari (1984). Molinari (1984) found scarps for the 1932 event as high as 1.4 m and as much as 2 m of dextral slip; he also found evidence for two additional Holocene events and at least three and possibly five or six surface faulting events during the latest Pleistocene and Holocene. The faulting style was principally dextral slip with tensional components and normal components in an en echelon pattern. According to Richter (1958) the faulting is consistent with dextral slip on a fault underlying Gabbs Valley, but not reaching the surface as a continuous break. Richter (1958) assumed the orientation of the buried fault was parallel to the trend of the rupture belt (i.e., N21°W).

Fallon–Stillwater–Rainbow Mountain earthquakes of July–August 1954

Three large earthquakes occurred one and a half months apart on the same fault. The first two events, a main shock (M = 6.8 and maximum MMI = IX) and its aftershock, were on July 6, 1954. The epicenter was located on the main fault zone on the east edge of Rainbow Mountain in the Stillwater Range, 24 km southeast of Fallon, and was felt over portions of California and Nevada (337,000 km^2; Slemmons and others, 1965). The third major event (M = 6.8) occurred on August 24, 1954. The maximum MMI intensity for this event was VIII (Slemmons and others, 1965) or IX (Coffman and von Hake, 1973); it was felt over 388,000 km^2, and there were instances of more severe damage than from the first shock (Slemmons and others, 1965; Steinbrugge and Moran, 1956).

These earthquakes produced discontinuous normal faulting along a NNE-trending fault bounding the eastern border of Rainbow Mountain (24 km east of Fallon) northward to the southern edge of the Carson Sink (Slemmons, 1957a). The July 6 events produced a fresh scarp 0.03 to 0.3 m high, west side up, for 17.7 km through the alluvial apron at the base of Rainbow Mountain and into the desert flats to the north (Tocher, 1956). The August 23 rupture extended the break 22.5 km northward with scarps as high as 0.8 m and increased some of the July 6 offset to as much as 0.5 m. The observed normal faulting from these events is in contrast with the focal mechanisms, which indicate predominantly dextral and dextral-oblique slip on a nodal plane striking north-northwest (Table 2). Doser (1986) concluded on the basis of wave-form modeling that the July 6 main shock was composed of two subevents. The first subevent, at a depth of 10 km, exhibited a predominance of dextral slip. The second subevent, at a depth of 7 km, was predominantly normal slip. This result could explain why strike slip was not observed at the surface. Doser (1986) finds that the August event was composed of three subevents, all best fit by dextral oblique slip on a fault trending north-northwest (Table 2). Geodetic studies also suggest that these events had substantial dextral slip (Meister and others, 1968). Snay and others (1985), in an attempt to explain the geodetic data on the basis of a dislocation model of the four historic rupture zones in this area, find their model does not adequately fit the slip associated with the Rainbow Mountain earthquakes. Their models for this Rainbow Mountain fault range from predominantly dip slip to predominantly strike slip, but in all cases the fault length and width appears too large given the seismically determined magnitude. They suggest magma movement as an alternative explanation for the displacements on this fault.

Dixie Valley–Fairview Peak earthquakes, December 16, 1954

Two large earthquakes occurred on December 16, 1954, in the eastern part of Churchhill County, Nevada. These earthquakes were the magnitude 7.3 and 6.9 Fairview Peak and Dixie Valley events, respectively (Slemmons and others, 1965). The mainshock felt area (518,000 km^2) included all of Nevada and parts of California, Oregon, Idaho, Utah, and Arizona (Cloud, 1957). In the sparsely populated epicentral zone, the mainshock maximum intensity was MM IX, where it could be estimated, but damage to structures in nearby towns was only intensity VII. The epicenter of the first shock was near a system of fault breaks on the east side of Fairview Peak and in the Louderback Mountains. The second epicenter was near fault breakage along the western edge of Dixie Valley at the base of the Stillwater Range, 48 km north of the first event (Tocher, 1957).

The earthquakes of December 16, 1954, were accompanied by offsets along many faults in four main zones of a north-trending belt 96 km long by 32 km wide, mainly along normal faults of the Basin-Range type (Slemmons, 1957b). The maximum vertical slip was 3.7 m at Bell Flat on the east side of Fairview Range. Significant strike-slip motion, amounting to 3.7 m of dextral slip, was also observed at Fairview Peak. Dip-slip displacements were prevalent in the northern part of the area, and oblique-slip or strike-slip displacements characterized the southern part.

Doser (1986) finds the seismic data for the Fairview Peak event best fit by three subevents occurring on a fault striking N10°W with predominantly dextral slip (Table 2). Snay and others (1985) find that the geodetic data in this region are consistent with slip on two separate planes for the Fairview Peak earthquake. A shallow dextral-oblique fault extends to 5 km depth and strikes N12°E, while the buried fault extends from 2 to 20 km depth, strikes N13°W, and is predominantly dip slip. Seismic and geodetic data for the Dixie Valley event are consistent with normal slip on a fault with strike of N10°W (Doser, 1986) or N6°E (Snay and others, 1985). Studies of microearthquakes in this region (Westphal and Lang, 1967; Stauder and Ryall, 1967; and Smith and others, 1972) indicated activity continuing along both north-south epicentral trends and northeast-trending zones (Table 2). Microearthquake focal mechanisms displayed both pure normal faulting along the northeast trends and oblique dextral slip along the north-trending zones.

OTHER SIGNIFICANT SEISMICITY

The Sierra Nevada–Great Basin boundary zone and the 1872 Owens Valley earthquake

This seismic zone follows the boundary region between the Sierra Nevada and the Great Basin. The earthquakes form a nearly continuous northwest-trending zone (Fig. 1). The breadth of this zone and the clustering of numerous earthquakes in several areas suggest activity on multiple faults. In the northern part of the zone near Reno (Fig. 1), clusters of earthquakes are observed in the following areas: (1) on the California-Nevada border west of Reno, where magnitude 6 events occurred twice in 1914 and once in 1948 (new work by Priestley, written communication, 1988, suggests that the largest of these events was east of Reno); a magnitude 5.6 earthquake produced surface faulting in 1950 along the Fort Sage Mountain fault in the northern Walker Lane belt (Slemmons, 1967); (2) southwest of Reno on the California-Nevada border, near the presumed location of the 1857 earthquake (Real and others, 1978); (3) north of Truckee, California, where an $M_L = 6.0$ shock occurred in 1966; (4) south of Reno in the Steamboat Hot Springs area; and (5) in the Virginia Range southeast of Reno. This band of activity continues to the northwest, into California, where several major seismic trends are apparent that may be associated with the Dog Valley, Mohawk Valley, Grizzly Valley, and Last Chance fault zones (Hawkins and others, 1986). Ryall (1977) suggests, on the basis of the long linear epicentral trends and their close association with the Sierra Nevadan range-front faults that the SNGBZ is a likely location for a major (M = 7+) earthquake. The largest event within the SNGBZ occurred in Owens Valley in 1872; on the basis of geologic data, it was estimated to be M = 7.5 to 7.8 (Beanland and Clark, 1987; Hanks and Kanamori, 1979), and on the basis of felt area, M = 8.0 (Oakeshott and others, 1972).

Mammoth

At the junction of the central Nevada seismic belt and the Sierra Nevada–Great Basin boundary zone (SNGBZ), earthquake swarms occur frequently in the area north of Bishop, and a major swarm near Mammoth Lakes has been in progress since October 1978. Through 1988, the Mammoth Lakes sequence has produced seven earthquakes with magnitudes greater than 6. Uplift, spasmodic tremor, and increased fumarole activity have also occurred in Long Valley caldera and likely are associated with magma injection (Ryall and Ryall, 1981, 1983; Savage and Clark, 1982; Miller and others, 1982). This zone has had the highest level of seismic activity since 1980. Savage and Cockerham (1987) suggested that the $M \leqslant 5.5$ events occur in a quasi-periodic fashion with an average interval of 18 months. As noted by Smith and Priestley (1988), however, the Chalfant Valley earthquake, to the north of Bishop, is an exception to this observation because aftershocks continued for more than six months after the mainshock. The causes of seismicity in this region are uncertain, but the proximity of Long Valley caldera and the intimate association of volcanic processes is a likely factor (Hill and others, 1985).

Caliente/Clover Mountains earthquake, 1966

This earthquake series deserves special mention because it is the largest earthquake (M = 5.7 to 6.1, University of California, Berkeley seismograph station) to occur in the southern Nevada Transverse Zone. The earthquake was accompanied by an aftershock swarm, which at its peak produced more than 8,000 events per day (Boucher and others, 1967). Page (1968) reports the depths of the aftershocks to be less than 9 km. Some of the aftershocks were relocated by Beck (1970) and Rogers and others (1983). In the latter study, a selected subset of the best-recorded aftershocks and the main shock were relocated using the joint-hypocenter relocation technique (Dewey and Spence, 1979). These relocated events occupied a NNE—trending zone 22 km long and 8 km wide on the southern end of the Clover Mountains. Based on the aftershock trend and several focal mechanisms for the main shock (Wallace and others, 1983; Smith and Lindh, 1978). Rogers and others (1983) infer dextral slip on a north-trending fault for this event.

Induced seismicity

Earthquakes have been induced by the activities of man at two locations in Nevada—the Nevada Test Site and Lake Mead. Tectonic stress apparently has been released as a result of underground nuclear explosions at the Nevada Test Site (NTS). This stress release is seen as surface displacements occurring at the time of the event (McKeown, 1975), as seismic energy release concurrent with the detonations, and as numerous aftershock earthquakes outside the zones of shattering. Hamilton and Healy (1969), Boucher and others (1969), Smith and others (1971), and Rogers and others (1977) presented evidence that numerous aftershocks followed the detonation of high-yield nuclear devices at NTS and the Central Nevada Test Area (CNTA); some of these earthquakes have had magnitudes $\simeq 5$. Based on these studies it appears that nuclear tests of at least $m_b \geqslant 5$ (Boucher and others, 1969) are required to trigger stress release in the form of aftershocks, although there may be exceptions, and the thresholds may vary between test areas (i.e., Pahute Mesa, Rainier Mesa, Buckboard Mesa, Yucca Flats, and Hot Creek Valley [CNTA]; Rogers and others, 1977). The tectonic energy that is released seismically at the time of the explosion and the seismic energy released in aftershocks have comparable values. The magnitude values equivalent to this energy release range between approximately the magnitude of the nuclear test and one magnitude unit less than that of the explosion (Aki and others, 1969; Aki and Tsai, 1972; Wallace and others, 1983; Lay and others, 1984; Wallace and others, 1985; Wallace and others, 1986). Bucknam (1969), McKeown and Dickey (1969), Orkild and other (1969), Maldonado (1977a, b), Snyder (1971, 1973), and Morris (1971), in studies of faults near nuclear tests, found that these events can generate vertical and horizontal displacements on existing tectonic faults that are produced with the first arrival of the explosion-generated seismic waves. As much as 100 cm of vertical displacement and 15 cm of horizontal dextral slip have been observed on faults as great as 10 km in length.

Hamilton and others (1971) noted that 95 percent of the aftershocks of four nuclear explosions having magnitudes greater than about 5.8 occurred within 14 km of ground zero, and 94 percent occurred in the upper 5 km of the crust. Rogers and others (1977) conducted similar studies for eight nuclear tests in the high-yield nuclear-test series about six years after the earlier series and found that, although the aftershocks in the latter testing series clustered more closely around ground zero, the depths of the aftershocks appeared to be significantly greater than the earlier study. Between 93 and 100 percent of the aftershocks occurred within 6 km of ground zero, and at least 95 percent of the hypocenters occurred between 4 and 10 km. These earthquakes do not clearly align with known faults in most cases, but they do sometimes exhibit north to north-northeast trends. Depth sections of the alignments suggest that nuclear-induced seismicity occurs on steeply dipping faults, and based on focal mechanisms, slip style ranges from strike slip on north-trending faults to dip slip on NNE-trending faults.

During and following the impoundment of Lake Mead, numerous earthquakes occurred; some of these events had magnitudes as great as 5 (Mead and Carder, 1941; Rogers and Lee, 1976). Rogers and Lee (1976) suggested that these earthquakes were caused by increases in pore pressure and hydrostatic head along existing faults of about 3 to 6 bars; they showed that the expected energy release resulting from this pore-pressure increase was the same order of magnitude as the total seismic energy release of earthquakes in the Lake Mead area. Earthquakes at Lake Mead occur from near-surface to about 12 km, and clusters appear to occur on steep faults, with slip style varying from strike slip on north-trending faults to dip slip on north-northeast– to northeast-trending faults. Activity rates and the maximum magnitudes of earthquakes occurring at Lake Mead have declined with time, suggesting partial relaxation of stress in the crust in the immediate vicinity of the lake. In 1988 renewed activity, including numerous felt earthquakes, occurred southwest of Hoover Dam (S. C. Harmsen, written communication, 1988).

SEISMIC GAPS

Wallace (1978) has noted that three seismic gaps may exist within the CNSB. These gaps, which are likely candidates for future large earthquakes (Figs. 1 and 3), are the Stillwater gap that lies between the 1954 and 1915 ruptures (Wallace and Whitney, 1984), the White Mountains gap between the 1872 and 1932 zones, and the southern Owens Valley gap that is south of the 1872 rupture. The White Mountains seismic gap has been identified as an area in which the next major earthquake in the western Great Basin has a high likelihood of occurring, and increased seismicity in and around the White Mountains gap may be precursory to such an event (Ryall and Ryall, 1983).

Thenhaus and Barnhard (1989) discuss the characteristics of previously recognized (Stewart, 1980) east-west zones of accommodation that bound northerly trending bands of seismicity, zones of like-age faulting, and domains of range tilt. Thenhaus and Barnhard suggest that an additional seismic gap, which they term the Sonoma Range gap, may lie between the northern terminus of the Pleasant Valley historic rupture zone and the northernmost accommodation zone (Fig. 1).

Some of these gaps, as defined by the present-day seismicity, appear shorter than the rupture-defined gaps (Figs. 1 and 2). That is, small- to moderate-magnitude earthquakes appear to extend into parts of the rupture-defined gaps. For example, there are a few scattered events in the Stillwater Gap, just north of the 1954 rupture zone. Although Gumper and Scholz (1971) first commented on the White Mountains gap, since then, earthquakes have occurred at its north end near the Excelsior Mountains, and also east of Mono Lake. The gap appears to be shortened on the south by the 1986 Chalfant Valley earthquakes (Cockerham and Corbett, 1987; Smith and Priestley, 1988). These events occurred north of the termination of the 1872 ruptures. Thus, the White Mountains seismicity gap is now only half the length of the White Mountains rupture gap. Ryall and Priestley (1975) suggested that high seismicity in the Excelsior Mountains may indicate that stress is released by a continuing series of small to moderate earthquakes and fault creep and that rupture of the northern segment of the White Mountains gap is less likely than it would be otherwise.

Inactivity on the northwest-trending Death Valley–Furnace Creek fault zone is a paradox because, although numerous Holocene scarps exist on these faults, suggesting that they are active (Hunt and Mabey, 1966; G. E. Brogan, written communication, 1979), little or no historic seismicity has occurred in this region that can be associated with these faults (Real and others, 1978; Rogers and others, 1987). Thus, this fault zone could be in the part of the seismic cycle in which the faults have experienced stress release in the recent geologic past. The alternative hypothesis—that the fault is locked and accumulating stress for the next event—appears to have less merit. Based on geologic and seismic data, Rogers and others (1983, 1987) inferred a clockwise horizontal principal-stress rotation eastward across the zone and suggested that, if the fault were locked and highly stressed, the stress orientations on both sides of the fault could be expected to be approximately equal. The inferred stress difference on either side of this structure could be indirect evidence that this fault zone is presently in a low-stress state.

Astiz and Allen (1983) suggested that the eastern section of the Garlock fault, which bounds the Great Basin, is a seismic gap. Clear evidence of Holocene displacement exists for this structure, yet very few earthquakes have occurred there in the historic record. Because the western half of the fault exhibits the youngest offsets, active creep, and low-level seismicity, while the eastern section appears locked, Astiz and Allen (1983) believe the eastern section of the Garlock has the greatest potential for a large earthquake.

FREQUENCY OF LARGE HISTORIC EVENTS

As noted by Ryall (1977), the time between large events in the historical record for Nevada ranges from 4 minutes to 43 years. Our understanding of earthquake recurrence in this region is confounded by inconsistencies between projected rates of large events from low- or intermediate-magnitude earthquake occurrence, the rate of occurrence of historic large-magnitude events, and the rate of occurrence of large-magnitude events predicted from geological studies. The wide disparity between these rates is evident in Table 3. The rates from Algermissen and others (1982) are based on their maximum-likelihood estimates (Bender, 1983) and historic seismicity in their zones 31, 32, 33; these zones represent the CNSB, but exclude the SNGBZ. This estimating procedure tends to heavily weight the intermediate-magnitude events, and reduces the influence of the large historic events, which accounts for part of the discrepancy between A and B in Table 3. There are, however, substantial differences in the rates of large events forecast on the basis of geologic data compared to those based on seismic data. The mean seismic rates (Table 3, B) exceed the mean geologic rates (Table 3, C). These differences can be qualitatively explained by a model of Great Basin earthquake occurrence discussed by Wallace (1987).

Based on studies of range-front faults in Nevada, Wallace (1987) suggests that clusters of events may occur on individual segments of a fault during an active period lasting hundreds to thousands of years. The active period is followed by quiescence for 10,000 to 30,000 years. Other segments of the same fault may or may not be active at the same time, but once active, these segments follow the same pattern. This model may extend to subzones of the Great Basin, as observed by Buckham and others (1980) in western Utah. Some subzones of that region display late Quaternary, but not Holocene faulting or the converse. Subzones can be expected to turn on for periods of hundreds to thousands of years, then become dormant while other subzones are active. This model appears consistent with the historic record of seismicity in the CNSB where several colinear fault segments became active almost simultaneously. In fact, most of west-central Nevada, where Holocene displacements have been observed on many range-front faults, may be part of a subzone in the active phase (Wallace, 1984a).

As noted by Wallace (1987), the temporal behavior of Great Basin events (here taken to be $M \geqslant 7.0$) complicates the assessment of the seismic hazard in the region. Use of the mean

TABLE 3. RATES OF LARGE ($M \geq 7.0$) EARTHQUAKE OCCURRENCE IN THE NEVADA SEISMIC ZONE

Source of Data (Assumption)	Return Period (years)
A. Historic seismicity (M≥7; all within the CNSB)	27
B. Projected seismic rates (CNSB)*	1,080
C. Geologic (Mean RP, Fully Cycle, SF)†	5,000-10,000
D. Geologic (Mean RP, Active Period, SF)†	1,500-3,000
E. Geologic (Quiet Period, SF)†	(No events)
F. Geologic (Mean RP, Active Period, CNSB incl. gaps))	300-1,500

Note: Abbreviations used are SF = single fault, RP = return period, and CNSB = Central Nevada Seismic Belt.

*Algermissen and others (1982). The rate for their zones 31, 32, and 33 combined is proportioned to the area of the CNSB (1.22×10^4 km^2).

†Wallace (1987)

rate of occurrence of large events (determined from geologic data; Table 3, C) overestimates the hazard on a fault segment if the short-term forecast extrapolates from the active period into the quiescent period and underestimates the hazard if the short-term forecast extrapolates from the quiescent period into the active period.

Estimating the rate of occurrence of large events over a region such as the CNSB is also problematic. The principal difficulty lies in the lack of enough geologic data to estimate the number of faults in the CNSB capable of producing large events, the ages of slip events on these faults, the time since the last slip event, and the duration of the active and dormant periods. Although these data are lacking for most CNSB faults, it is possible, nonetheless, to estimate a rate for large events under certain assumptions that are based on the patterns of fault behavior that Wallace has observed. If we assume, for instance, that one full cycle, including the active and dormant phases for a single fault segment, lasts 15,000 to 30,000 years and that, on average, three large events occur during the active phase (5,000 to 10,000 years), then the mean return period over a full cycle is 10,000 years (Table 3, C; Wallace, 1987). Following similar reasoning, the mean return period over the active period is 1,500 to 3,000 years (Wallace, 1987). If we assume that six segments (including gaps) exist in the CNSB that are capable of producing large events, then the mean return period for CNSB large events during the active period is 300 to 1,500 years (Table 3, F). Notably, this return-period range brackets the return period projected by the intermediate-level seismicity (Table 3, B).

Furthermore, it has also been suggested that seismic strain in some regions may be released in a "characteristic earthquake" on each major fault segment, such that a zone might have only low-level seismicity before and after a characteristic earthquake, with few or no events in the magnitude range 5 to 7 (Schwartz and Coppersmith, 1984). In this scenario the recurrence curve would be discontinuous with a rate spike above magnitude 7.

TABLE 4. SEISMIC RATES IN NEVADA

Zones*/ Area (10^4 km^2)	Area and approximate age of faulting†	Return period for M≥7.0 (years)	Annual rate of exceedance per 10^4 km^2 M≥6.4	M≥7.0	M^*_{max}
31/ 4.71	NSZ, excluding historic rupture zone, Holocene	280	2.6×10^{-3}	7.6×10^{-4}	7.6
31, 32, 33/ 6.16	NSZ, including historic rupture zone, Holocene	210	2.6×10^{-3}	7.6×10^{-4}	7.6
31, 32, 33, 29/ 7.99	Nevada seismic zone and the eastern Sierran front, Holocene	180	2.0×10^{-3}	6.8×10^{-4}	7.6
31, 32, 33, 34/ 16.2	Western Nevada, Holocene	170	1.3×10^{-3}	3.6×10^{-4}	7.6
17, 18, 19/ 12.6	Eastern/southern Nevada, late Quaternary	640	5.8×10^{-4}	1.2×10^{-4}	7.6

*Zones, rates, and maximum magnitudes are adapted from Algermissen and others (1982).
†Based on Wallace (1984a)

Thus, the difference in seismically inferred return periods given in Table 3, A and B, could be partially explained by this model, but could also be the result of "contagion" between fault segments. That is, once rupture occurs in an active zone, other nearby fault segments rupture over short periods of time (Perkins, 1987), perhaps due to increased loading of segments adjacent to the ruptured segment.

As a means of comparing seismic rates for various areas of Nevada, rates of seismicity from Algermissen and others (1982) for several geologic subzones of the Great Basin are shown in Table 4. The logarithm of the number of events, N, versus magnitude, M, can be fit with lines of the form

$$\log N = a - bM. \quad (1)$$

These lines have slopes (b-values) for Nevada seismic zones varying from about 0.9 to 1.1, although b-values as great as 1.5 to 2.0 have been observed in the regions of induced seismicity at the Nevada Test Site (NTS) and Lake Mead (Hamilton and others, 1971; Rogers and others, 1977, Rogers and Lee, 1976). Recurrence slopes are not well determined for some regions of Nevada, particularly east and south of the CNSB, because of the low level of earthquake occurrence. The completeness of the earthquake record for Nevada is not well determined, and is likely to be a function of both time and geographic position. The record is likely most complete for the region near Reno, where the instrumental record is longest. Rogers and others (1977) estimated completeness for a large portion of Nevada, including most of the CNSB. They evaluated the time period from 1845 to 1974 and a region that included a substantial portion of southern California. Their results for this region suggest that earthquakes with magnitudes ranging between 4 and 5, 5 and 6, 6 and 7, and 7 and 8 are complete for the most recent 40, 50, 60, and 130 years, respectively.

Ryall and Priestley (1975) plotted the number of earthquakes occurring in the epicentral zones of large Nevada earthquakes versus time since the main shock and found that the logarithm of the number of events was linearly related to the time since the last large event in that region. They conclude that the aftershocks effectively die out about a century after the mainshock.

EARTHQUAKE DEPTH DISTRIBUTIONS IN THE GREAT BASIN

Accurate estimates of focal depth are an important factor in integrating seismicity with tectonic models. The most accurate depth estimates are likely to derive from dense network data with stations that are within one focal depth of the earthquake, for events within the perimeter of the network. In addition, however, accurate crustal models are required, and the location procedure should include at least five P-wave phase readings and one or more S-wave readings. Because data used to locate earthquakes are typically from stations more than one focal depth from the epicenter, earthquake focal depth is frequently poorly constrained. In general, the most accurate earthquake depths for this region have been obtained from data derived from detailed microearthquake surveys and telemetered local networks. Such studies have been conducted in Nevada by Oliver and others (1966), Westphal and Lange (1967), Stauder and Ryall (1967), Ryall and Savage (1969), Gumper and Scholz (1971), Ryall and Malone (1971), Hamilton and others (1971), Smith and others (1971), Fischer and others (1972), Papanek and Hamilton (1972), Ryall and Priestley (1975), Rogers and Lee (1976), Rogers and others (1977), Ryall and Vetter (1982), Tarr and Rogers (1986), and Rogers and others (1987). Although considerable additional study of individual active zones will be necessary before confidence can be acquired concerning earthquake depths in this region, hypocenters appear to display some consistent general characteristics.

Great Basin earthquakes are rarely deeper than 20 km. For most seismic zones in the Great Basin, more than 95 percent of the events occur in the upper 15 km (Ryall and Savage, 1969; Rogers and others, 1987). Within the upper 15 km of the crust, hypocenter concentrations display considerable variability (Fig. 5; Stauder and Ryall, 1967; Ryall and Savage, 1969; Okaya and Thompson, 1985; Richins and others, 1985). Modal depths of background microearthquakes or aftershocks may occur at any depth between about 1 and 15 km. In contrast, mainshock focal depth occurs in the range 8 to 16 km for the best-determined values (Doser and Smith, 1985; Doser, 1986, 1987, 1988; Baker and Doser, 1988). This observation has been one of the chief arguments supporting the existence of a brittle-ductile crustal boundary at this depth in the Great Basin (Anderson, 1971; Tocher, 1975; Smith and Bruhn, 1984). Because mainshock events commonly initiate near the base of the brittle upper crust between 10 and 15 km, Smith and Bruhn (1984) infer that maximum strength of the brittle crust occurs at the brittle-ductile boundary.

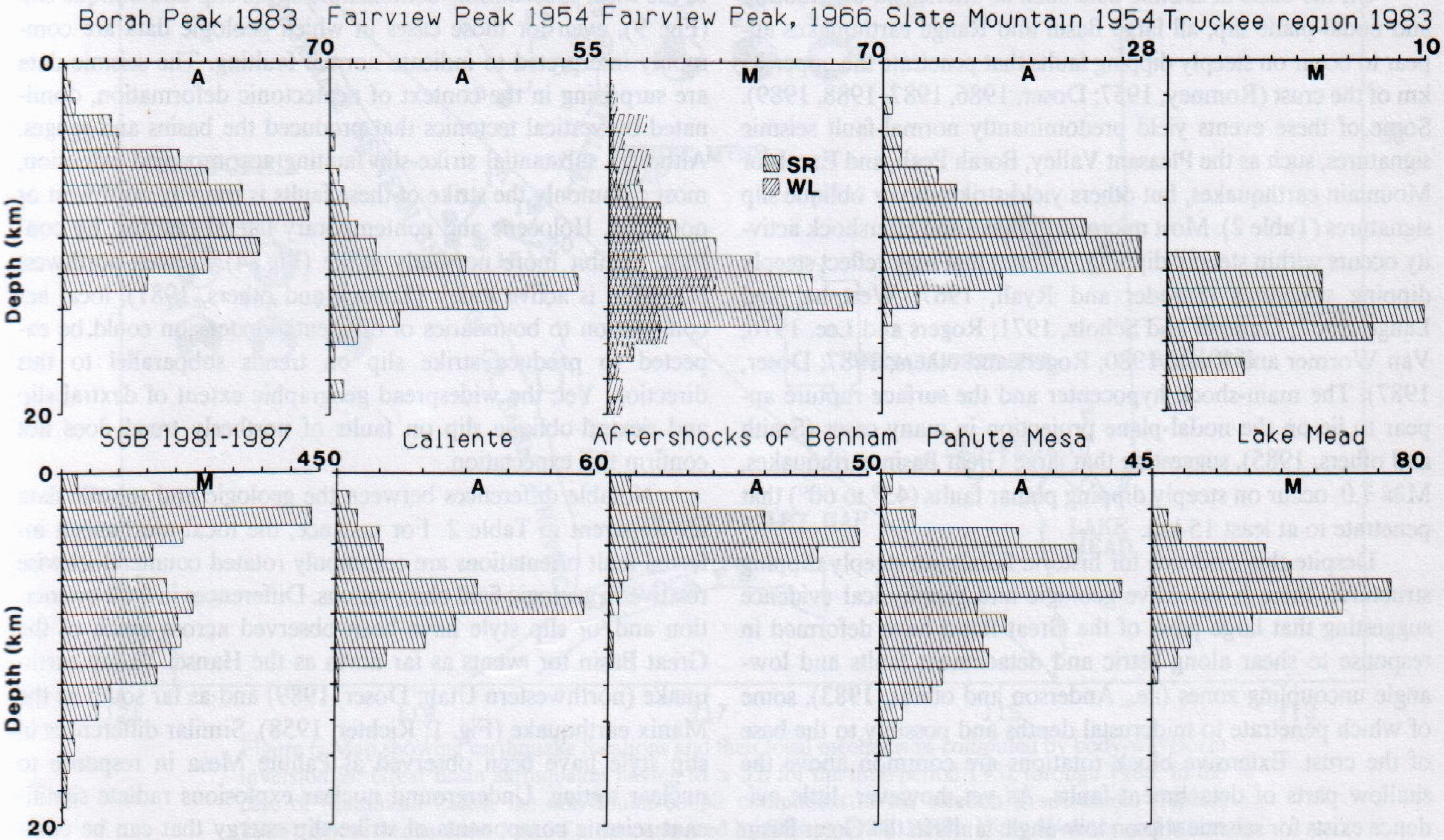

Figure 5. Depth-of-focus histograms for aftershock studies (labeled A) and microearthquake studies (labeled M) for various regions in the Great Basin. We plot numbers of earthquakes versus depth of focus for events in the range 0.0 to 20.0 km. For all but one of the data sets, less than 1 percent of the estimated depths are greater than 20 km. About 8 percent of the Fairview Peak depths computed by Westphal and Lange (1967) are greater than 20 km. References are: Borah Peak 1983—Charley Langer (written communication, 1987); Fairview Peak 1954, Slate Mountain 1954, and Caliente 1966—Ryall and Savage (1969); Fairview Peak 1966—Stauder and Ryall (SR) (1967) and Westphal and Lange (WL) (1967); Truckee region 1983—Hawkins and others (1986); southern Great Basin (SGB)—Rogers and others (1987) and Harmsen and Rogers (1987); Benham and other Nevada Test Site (NTS) nuclear test aftershocks—Hamilton and others (1971); aftershocks of Pahute Mesa (NTS) nuclear tests of 1976—Rogers and others (1977); and Lake Mead earthquakes of 1972 and 1973—Rogers and Lee (1976). Depths are relative to the mean surface level for each study area.

Hypocentral distributions for small-earthquake series fall into several categories. Some events occur in weakly tabular or cylindrical clusters over depth ranges of only several kilometers (Stauder and Ryall, 1967; Fischer and others, 1972; Hawkins and others, 1986; Arabasz and Julanders, 1986; Rogers and others, 1987). In other cases, clusters of microearthquakes appear to occur in steeply plunging cylindrical or tabular volumes of rock extending from near-surface to 10 to 15 km (Rogers and Lee, 1976; Rogers and others, 1987). Although these patterns may be questioned on the basis of known focal depth errors, the patterns have been observed in several cases using tightly clustered stations (i.e., Hamilton and others, 1971; Rogers and Lee, 1976; Rogers and others, 1987). In some cases this appearance may be an artifact of location error; nonetheless, this feature of microearthquake occurrence has been noted in studies of well-located earthquakes from dense arrays, leading Rogers and others (1987) to suggest that the cylindrical clusters may be real and represent failure in weak rock along the intersection of faults.

On the basis of seismic data such as aftershock distribution and nodal-plane dip, all large Basin and Range earthquakes appear to occur on steeply dipping faults that penetrate the upper 15 km of the crust (Romney, 1957; Doser, 1986, 1987, 1988, 1989). Some of these events yield predominantly normal-fault seismic signatures, such as the Pleasant Valley, Borah Peak, and Excelsior Mountain earthquakes, but others yield strike-slip or oblique slip signatures (Table 2). Most microearthquake and aftershock activity occurs within steeply dipping volumes that may reflect steeply dipping structures (Stauder and Ryall, 1967; Westphal and Lange, 1967; Gumper and Scholz, 1971; Rogers and Lee, 1976; Van Wormer and Ryall, 1980; Rogers and others, 1987; Doser, 1987). The main-shock hypocenter and the surface rupture appear to lie on the nodal-plane projection in many cases (Smith and others, 1985), suggesting that large Great Basin earthquakes, $M \geqslant 7.0$, occur on steeply dipping planar faults (45° to 60°) that penetrate to at least 15 km.

Despite this evidence for historic failure on steeply dipping structures, there is extensive geologic and geophysical evidence suggesting that large parts of the Great Basin have deformed in response to shear along listric and detachment faults and low-angle uncoupling zones (i.e., Anderson and others, 1983), some of which penetrate to midcrustal depths and possibly to the base of the crust. Extensive block rotations are common above the shallow parts of detachment faults. As yet, however, little evidence exists for seismic slip on low-angle faults in the Great Basin or in any other extensional regime (Jackson, 1987). Smith and Richins (1984) termed this problem the "paradox and paradigm" of Great Basin deformation. Although a small percentage of focal-mechanism nodal planes do have shallow dip (Figs. 6, 7, 8, 9), in many cases these low-angle nodal planes are likely to be auxiliary nodal planes. This conclusion is drawn on the basis of correlations between inferred principal-nodal planes and aftershock lineations and/or mapped structure in the southern Great Basin (Rogers and others, 1987).

Low-angle structures could be active aseismically. Eddington and others (1987) find that geodetically determined slip rates for extension of the Great Basin are about the same order of magnitude as the seismically inferred extensional slip rates and the slip rates estimated from geologic observations averaged over the Holocene (Minister and Jordan, 1987). Both the seismic and geologic estimates are based on the assumption of a predominance of normal slip on steeply dipping faults and nodal planes. Thus, aseismic slip on low-angle faults is not required to explain these observations.

FOCAL MECHANISMS AND TECTONICS

Figures 6 and 7 present the focal mechanism determinations that have been obtained for the largest Nevada earthquakes, as well as representative mechanisms determined for low-magnitude seismicity or microearthquakes (the data for these figures are presented in Appendix A, Tables A1 and A2). Table 2 compares fault parameters obtained from geologic and seismic data. Many of the focal mechanisms demonstrate strike slip and oblique slip (Fig. 9), even for those cases in which geologic data are commonly interpreted to indicate normal faulting. The seismic data are surprising in the context of neotectonic deformation, dominated by vertical tectonics that produced the basins and ranges. Although substantial strike-slip faulting accompanied extension, most commonly the strike of these faults is roughly northwest or northeast. Holocene and contemporary lateral faulting, by contrast, exhibit more northerly strike (Fig. 4). If west-northwest extension is active today (Zoback and others, 1981), local accomodation to boundaries of differential extension could be expected to produce strike slip on trends subparallel to this direction. Yet, the widespread geographic extent of dextral slip and dextral-oblique slip on faults of northerly trend does not confirm this expectation.

Notable differences between the geologic and seismic data are apparent in Table 2. For instance, the focal-mechanism inferred fault orientations are commonly rotated counterclockwise relative to geologic field observations. Differences in fault orientation and/or slip style have been observed across much of the Great Basin for events as far north as the Hansel Valley earthquake (northwestern Utah; Doser, 1989) and as far south as the Manix earthquake (Fig. 1; Richter, 1958). Similar differences in slip style have been observed at Pahute Mesa in response to nuclear testing. Underground nuclear explosions radiate significant seismic components of strike-slip energy that can be comparable in energy release to the explosion itself (i.e., Aki and Tsai, 1972), while producing predominantly vertical displacements on scarps at the surface.

Although differences are common between seismic and geologic observations, they seem to be in accord locally in some cases. For instance, in the southern Nevada transverse zone, Rogers and others (1987) find correlations in several locales between epicenter lineations, focal-mechanism nodal planes, and surrounding structural grain, suggesting northerly trending dextral slip and oblique and normal slip on northeasterly trending faults.

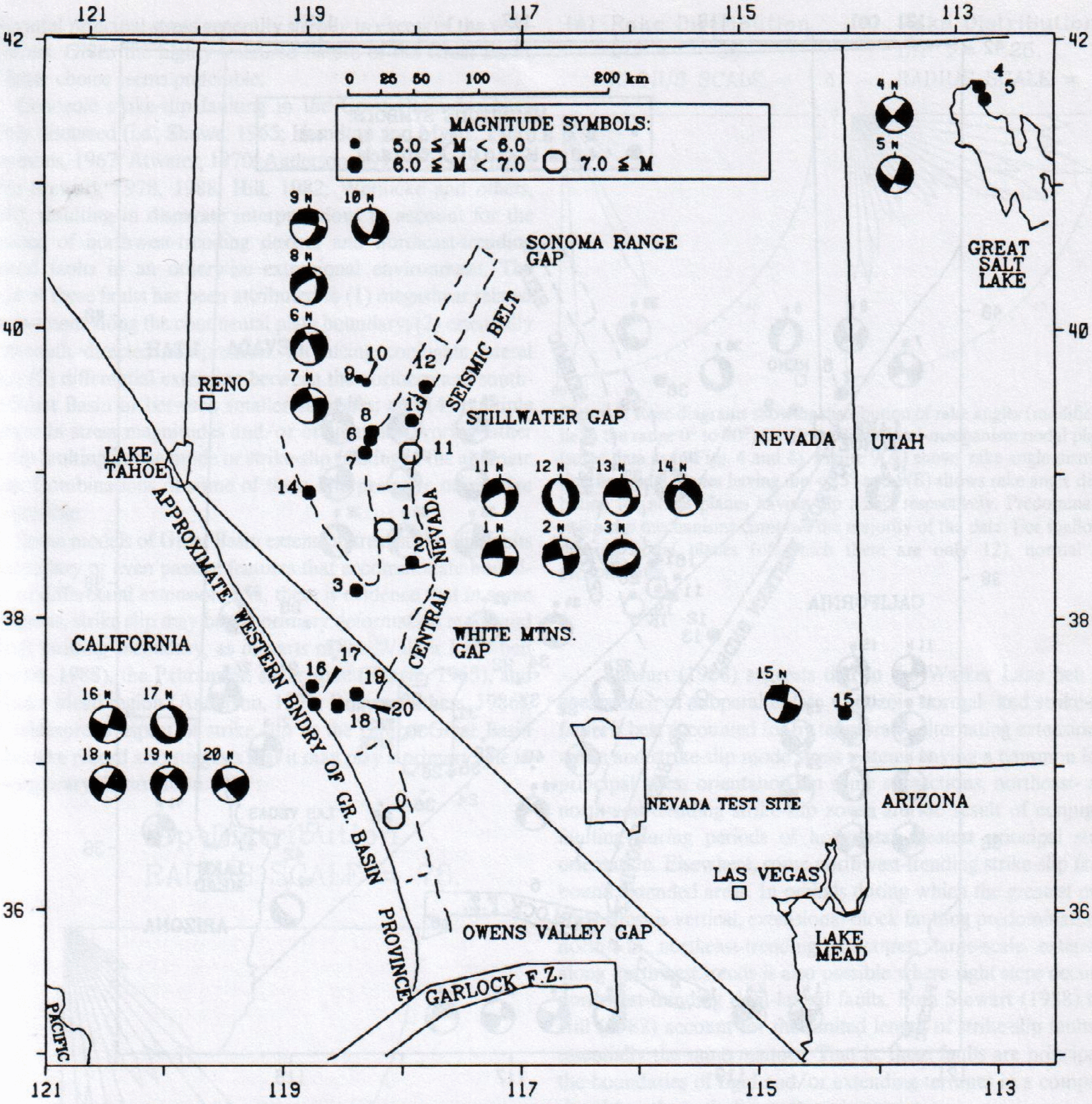

Figure 6. Map showing earthquake locations and their focal mechanisms computed by body-waveform inversion for Great Basin earthquakes having M ≥ 5.0 for the time period 1932 through 1986. In the case of Mammoth Lakes, the non-double-couple component of the solution is substantial (Sipkin, 1986). Focal mechanisms 1 to 14 were computed by Doser (1986, 1987), 15 by Wallace and others (1983), 16 and 17 by Sipkin (1986), 18 by Barker and Wallace (1986), 19 and 20 by Cockerham and Corbett (1987). Boundaries of central Nevada seismic belt from Wallace (1984a), and Garlock fault zone from Astiz and Allen (1983).

Anderson and Barnhard (1987), in a topical study of young deformation in the Sevier Valley, Utah, concluded there was a fair correspondence between late Quaternary strike-slip and normal faulting and deformation inferred from earthquake focal mechanism data (Arabasz and Julander, 1986).

Figure 10 shows the average T-axes (tension) orientations from earthquake focal mechanisms in various active areas of the Great Basin. Because both strike slip and normal slip are observed in most of these zones, the greatest horizontal principal stress and the vertical stress are inferred to be approximately equal (Zoback and Zoback, 1980). Rogers and others (1987) argue that these stress conditions are pervasive throughout the brittle crust (in the

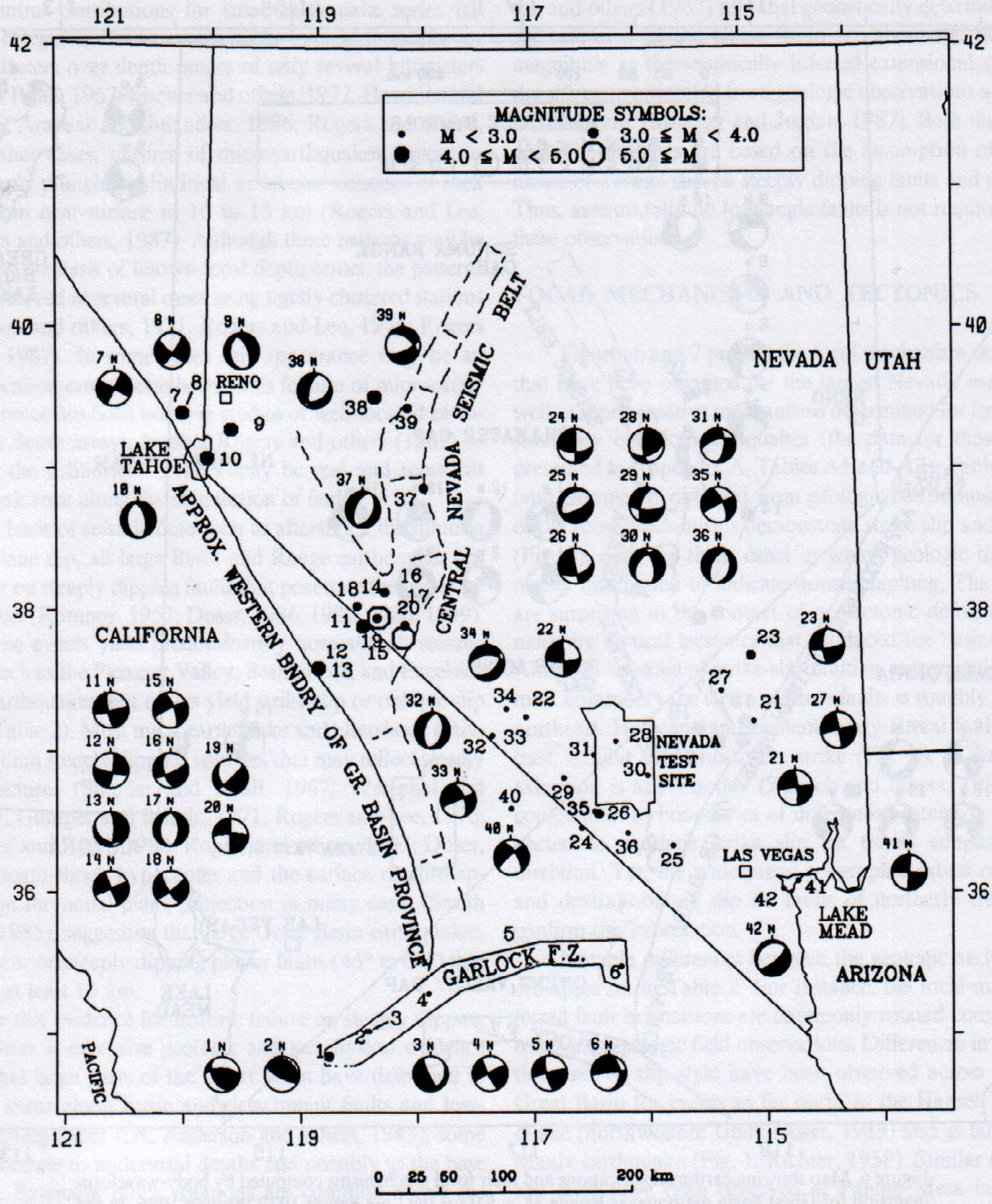

Figure 7. Map showing earthquake locations and their focal mechanisms computed from first-motion P-wave arrivals at local seismograph networks in the Great Basin and Garlock fault zone. Focal mechanisms 1 through 6 from Astiz and Allen (1983), 7 through 20 and 37 through 39 from Vetter and Ryall (1983) and Vetter (1984), 21 through 24 from Rogers and others (1987), and 25 through 36 and 40 from Harmsen and Rogers (1987).

southern Great Basin) because both styles of faulting are observed from near-surface to about 20 km. Figure 11 shows three cross sections with focal spheres in plan view, projected to the section plane at the depth of focus of each earthquake. This figure emphasizes the comingling of strike slip and normal faulting over the full depth range of earthquake occurrence. Harmsen and Rogers (1986) note that in a region where all fault orientations are available for slip, stress conditions of this type permit both slip styles with equal likelihood. In fact, based on the focal mechanisms, an apparent preference exists in the data sets for strike slip and oblique slip. It is unclear whether this preference is due to greater availability of certain fault strikes or whether it is due to a greatest horizontal principal stress generally slightly in excess of the vertical stress. Given the highly fractured nature of the Great Basin, the latter choice seems preferable.

Cenozoic strike-slip faulting in the Great Basin has been widely discussed (i.e., Shawe, 1965; Hamilton and Myers, 1966; Slemmons, 1967; Atwater, 1970; Anderson, 1971, 1973; Wright, 1976; Stewart, 1978, 1988; Hill, 1982; Wernicke and others, 1988), resulting in disparate interpretations to account for the presence of northwest-trending dextral and northeast-trending sinistral faults in an otherwise extensional environment. The origin of these faults has been attributed to (1) megashear related to movement along the continental plate boundary; (2) essentially north-south–directed compression, producing conjugate lateral faults; (3) differential extension between the northern and southern Great Basin or between smaller subzones; and (4) multiple changes in stress magnitudes and/or orientation favoring either dip-slip faulting in one mode or strike-slip faulting in the alternate mode. Combinations of some of these interpretative origins are also possible.

Some models of Great Basin extension treat strike-slip faults as secondary or even passive features that accommodate boundaries of differential extension. Yet, there is evidence that in some subregions, strike slip may be the primary deformation mode and normal faulting secondary, as in parts of the Walker Lane belt (Stewart, 1988), the Pahranagat shear zone (Shawe, 1965), and the Lake Mead region (Anderson, 1971; Ron and others, 1986). The widespread aspect of strike slip in the central Great Basin earthquake record also suggests that it may play a primary role in contemporary deformation.

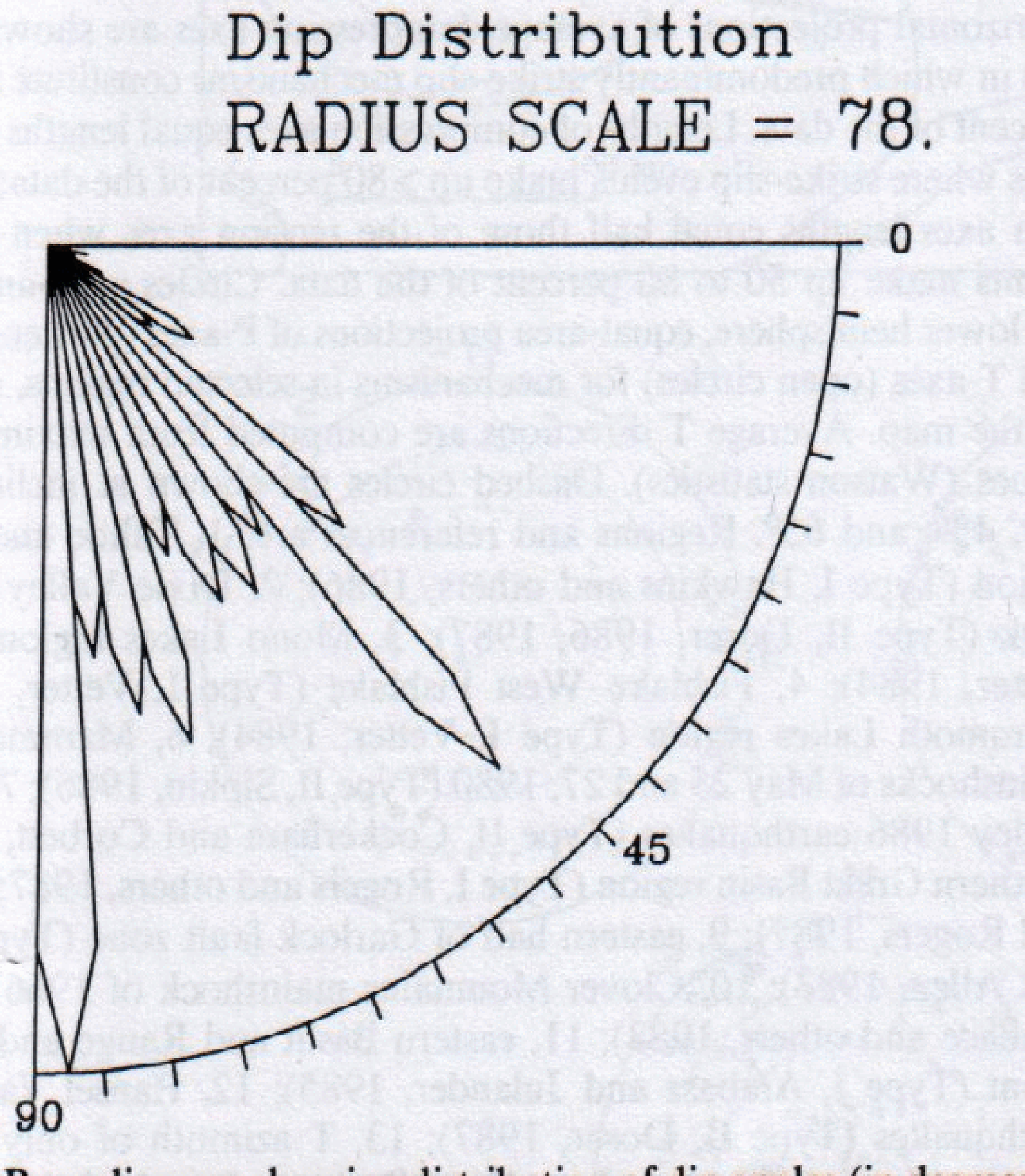

Figure 8. Rose diagram showing distribution of dip angles (in degrees) of Great Basin focal-mechanism nodal planes. The source regions for these data are shown in greater detail in Figure 9 below. We have not attempted to identify the preferred fault planes; thus, two dip angles per focal mechanism are included. The rose petal *lengths* (not areas) are proportional to the number of nodal plane dip angles in each 5° interval.

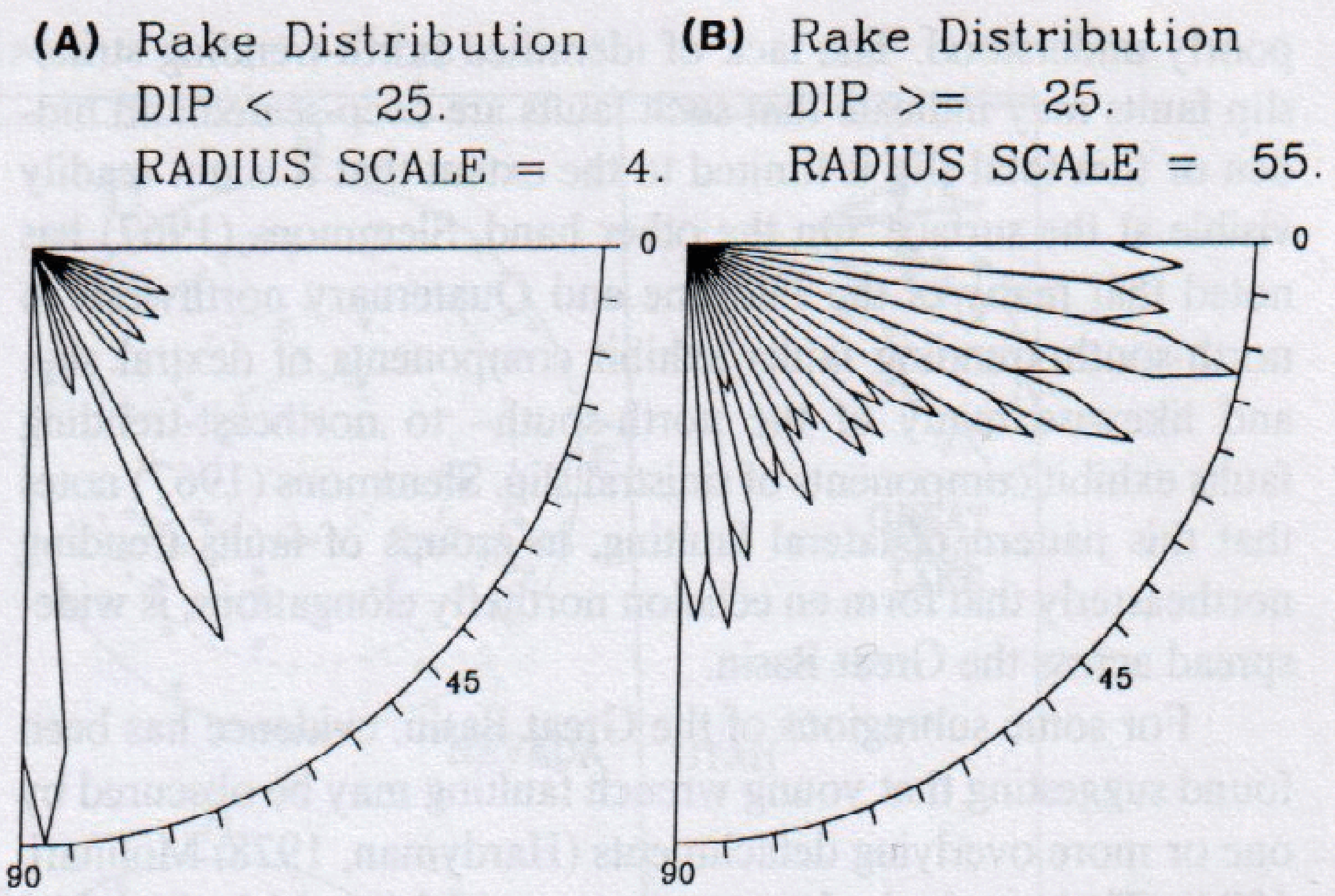

Figure 9. Rose diagrams showing distribution of rake angles (modified to lie in the range 0° to 90°) for Great Basin focal-mechanism nodal planes (same data as in Figs. 4 and 6). Figure 9(A) shows rake angle distribution for nodal planes having dip <25° and 9(B) shows rake angle distribution for nodal planes having dip ⩾25°, respectively. Predominantly strike-slip mechanisms compose the majority of the data. For shallowly dipping nodal planes (of which there are only 12), normal slip predominates.

Stewart (1988) suggests that in the Walker Lane belt the coexistence of subparallel late Cenozoic normal- and strike-slip faults is best accounted for by temporally alternating extensional-mode and strike-slip mode stress systems having a common least principal stress orientation. In some subsections, northeast- and northwest-trending strike-slip zones are the result of conjugate faulting during periods of horizontal greatest principal stress orientation. Elsewhere, some northwest-trending strike-slip faults bound extended areas. In periods during which the greatest principal stress is vertical, extensional block faulting predominates on north- to northeast-trending structures; large-scale extension along northwest trends is also possible where right steps occur in northwest-trending right-lateral faults. Both Stewart (1988) and Hill (1982) account for the limited length of strike-slip faults in essentially the same manner. That is, these faults are principally the boundaries of rigid and/or extending terranes in a compressional (north-south directed) environment.

It appears that contemporary strike-slip deformation, which on the basis of seismic data seems to occur primarily along northerly trending faults, differs substantially in orientation and geographic location from neotectonic faulting. Wright (1976) notes that Cenozoic strike-slip faults are most frequently observed in the boundary zones of the Great Basin. Although the western boundary zone may be large, as noted by Stewart (1988) in his description of the Walker Lane belt, seismicity data indicate that contemporary strike slip is observed outside the Walker Lane within the CNSB, across the southern Great Basin, and as far north and east as Hansel Valley, Utah.

The discrepancies in fault orientations and slip directions inferred from seismic and geologic data, where they occur, are poorly understood. The lack of identified north-trending strike-slip faults may indicate that such faults are deep-seated and hidden or that total slip is limited to the extent that it is not readily visible at the surface. On the other hand, Slemmons (1967) has noted that many of the Pliocene and Quaternary northwest- to north-south–trending faults exhibit components of dextral slip, and likewise many of the north-south- to northeast-trending faults exhibit components of sinistral slip. Slemmons (1967) notes that this pattern of lateral faulting, in groups of faults trending northeasterly that form en echelon northerly elongations, is widespread across the Great Basin.

For some subregions of the Great Basin, evidence has been found suggesting that young wrench faulting may be obscured by one or more overlying detachments (Hardyman, 1978; Molinari, 1984). Their geologic data support a model in which the initial stage of deep-seated horizontal shear may act to produce folding and sets of Reidel shears in a hypothesized detached upper-crustal plate. In this interpretation, observed surface displacements and block faulting are a response to deep-seated lateral shear. It is also possible, of course, that differences in geologic and seismic data are due to lack of detailed geologic investigations throughout the Great Basin of the kind conducted by Molinari (1984), Angelier and others (1985), and Anderson and Barnhard (1987).

One exception to the paucity of observable north-trending dextral faults is the faulting associated with the Owens Valley 1872 earthquake. Dextral slip appears to be the primary slip sense in this earthquake (Beanland and Clark, 1987); nearby, however, spectacular young range-front faults bound the eastern side of Owens Valley, but these faults were not activated by this event. The 1872 earthquake ruptured about 100 km of a north- to north-northwest–trending fault zone on the floor of Owens Valley with 4 to 10 m of displacement. Some secondary faults, such as the Lone Pine fault, had 1 to 2 m of vertical rupture (Lubetkin and Clark, 1987a). This example demonstrates that major contemporary strike-slip and late Quaternary normal faulting events can coexist within small subregions of the Great Basin (Zoback, 1989).

Another means of coping with discordance between contemporary and neotectonic deformation styles, is to argue that the region is presently subjected to a short-lived regional-stress field (Eaton and others, 1978). In principal, either the orientation or magnitudes of the principal stresses may exhibit temporal variation. Stress changes within the Tertiary have been inferred from the geologic record in selected locales (i.e., Donath, 1962; Wright, 1976; Anderson and Ekren, 1977; Angelier and others, 1985; Frizzell and Zoback, 1987), or for the Great Basin (Zoback and others, 1981; Stewart, 1988), lending credence to this possibility. Zoback and Beanland (1986a, b) and Zoback (1989) suggest that large fluctuations in the relative magnitudes of the principal stresses are required to account for the presence of both strike-slip and normal faulting in the Owens Valley–Sierran Front region in Pleistocene to Holocene time (Lubetkin and Clark, 1987b). Intraplate stress changes may be related to stress build-up and stress release along major faults of the continental plate margin and stress transfer to intervening faults, such as the Death Valley–Furnace Creek fault system, the Garlock fault, or other faults within the Walker Lane belt. In this way, contemporary intraplate deformation would be attributed to superposition of variable plate-boundary stresses with internal stresses such as back-arc extension (Zoback and others, 1981; Coney, 1987), gravitational collapse (Wernicke and others, 1988), or other mechanisms (Spencer and Chase, 1989); the relative influence of these two stresses as a function of time would be determined by factors such as the relative motion and coupling of the Pacific and North American plates.

Although it is possible to look to the plate boundary for an explanation of complexities and inconsistencies in the Great Basin, we favor the notion that forces internal to the province are responsible for contemporary deformation (Wernicke and others, 1987; Wernicke and others, 1988; Sonder and others, 1986; Jackson, 1987). For instance, the coexistence of strike-slip and normal faulting throughout the brittle crust (at least in the southern Great Basin) requires that the greatest horizontal stress increase with depth, leading to the conclusion that crustal stresses are consistent with a basal traction acting along the base of the crust or at the brittle-ductile boundary (McGarr, 1982; Rogers and others, 1987). Gumper and Scholz (1971) reached the same conclusion regarding deformation in this region, but on the basis

Figure 10. Map showing directions of average tension axes for focal-mechanism data collected from local network studies (Type I) or from large ($M > 6$) earthquake waveform inversion studies (Type II). Horizontal projections of average compression axes are shown for data sets in which predominantly strike-slip mechanisms constitute at least 50 percent of the data. Lengths of compression axes equal lengths of tension axes where strike-slip events make up ≥80 percent of the data; compression axes lengths equal half those of the tension axes when strike-slip events make up 50 to 80 percent of the data. Circles surrounding map are lower hemisphere, equal-area projections of P-axes (darkened circles) and T-axes (open circles) for mechanisms in selected regions, numbered on the map. Average T directions are computed from maximum eigen values (Watson statistics). Dashed circles are shown at inclinations of 25°, 45°, and 65°. Regions and references are: 1, Tahoe and Truckee region (Type I, Hawkins and others, 1986); 2, Dixie Valley–Fairview Peak (Type II, Doser, 1986, 1987); 3, Mono Lakes region (Type I, Vetter, 1984); 4, Fishlake–West Fishlake (Type I, Vetter, 1984); 5, Mammoth Lakes region (Type I, Vetter, 1984); 6, Mammoth Lakes mainshocks of May 25 and 27, 1980 (Type II, Sipkin, 1986); 7, Chalfant Valley 1986 earthquakes (Type II, Cockerham and Corbett, 1987); 8, southern Great Basin region (Type I, Rogers and others, 1987; Harmsen and Rogers, 1987); 9, eastern half of Garlock fault zone (Type I, Astiz and Allen, 1983); 10, Clover Mountains mainshock of 1966 (Type II, Wallace and others, 1983); 11, eastern Basin and Range and Wasatch Front (Type I, Arabasz and Julander, 1985); 12, Hansel Valley 1934 earthquakes (Type II, Doser, 1987); 13, T azimuth of only available focal mechanism for a southern Great Basin earthquake just west of the Death Valley fault trace (event 40, Figure 5); 14, Durrwood Meadows series of 1983 to 1984 (Type I, Jones and Dollar, 1986, their Table 2). The only regional data set showing predominantly normal-slip mechanisms is Durrwood Meadows in the Sierra Nevada, and thus not within the Great Basin.

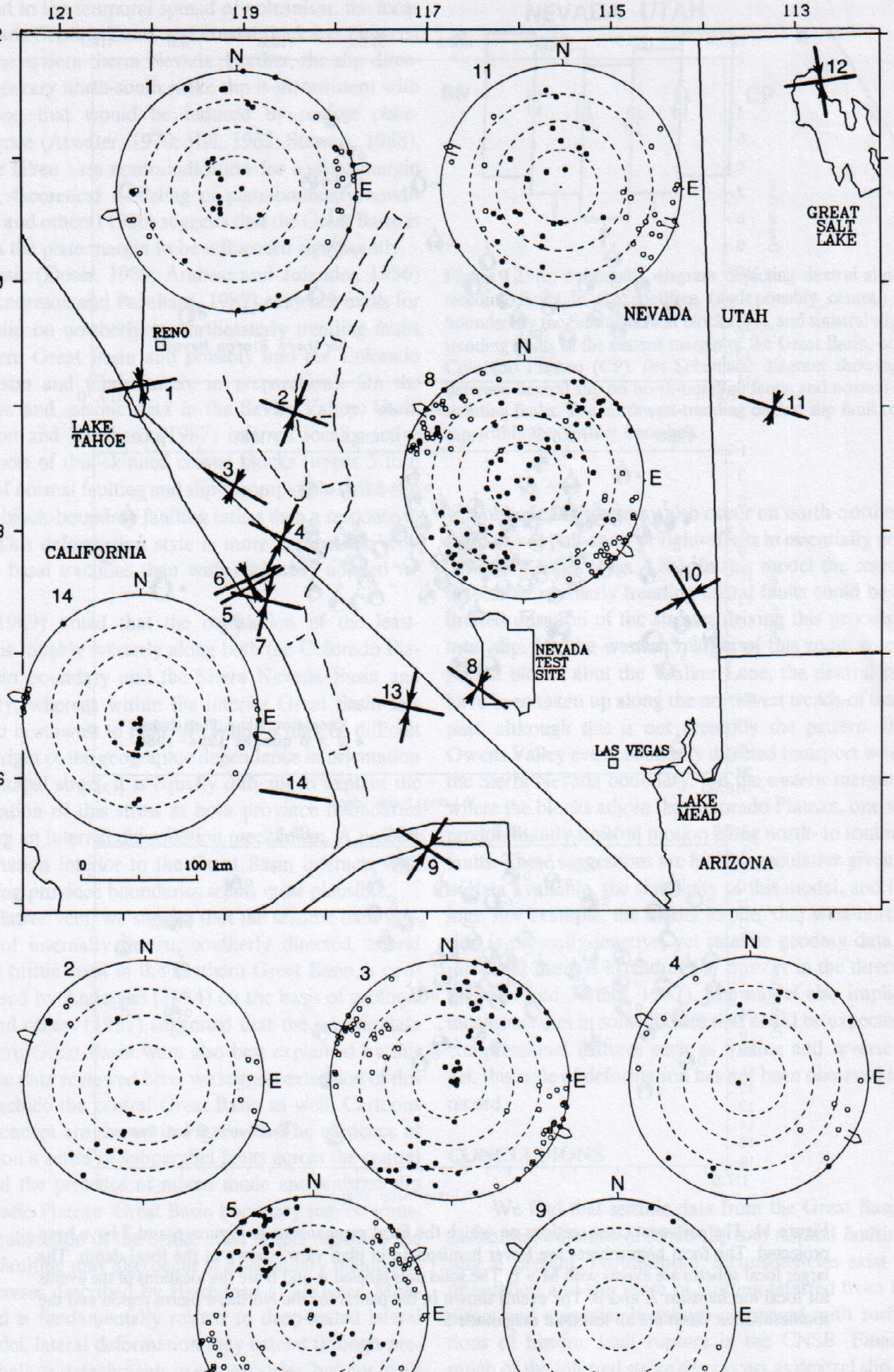
121
119
117
115
113
42
40
38
36
N
E
11
12
GREAT
SALT
LAKE
NEVADA
UTAH
RENO
LAKE
TAHOE
CALIFORNIA
NEVADA
TEST
SITE
LAS VEGAS
LAKE
MEAD
ARIZONA
100 km
1
2
3
4
5
6
8
9
10
13
14

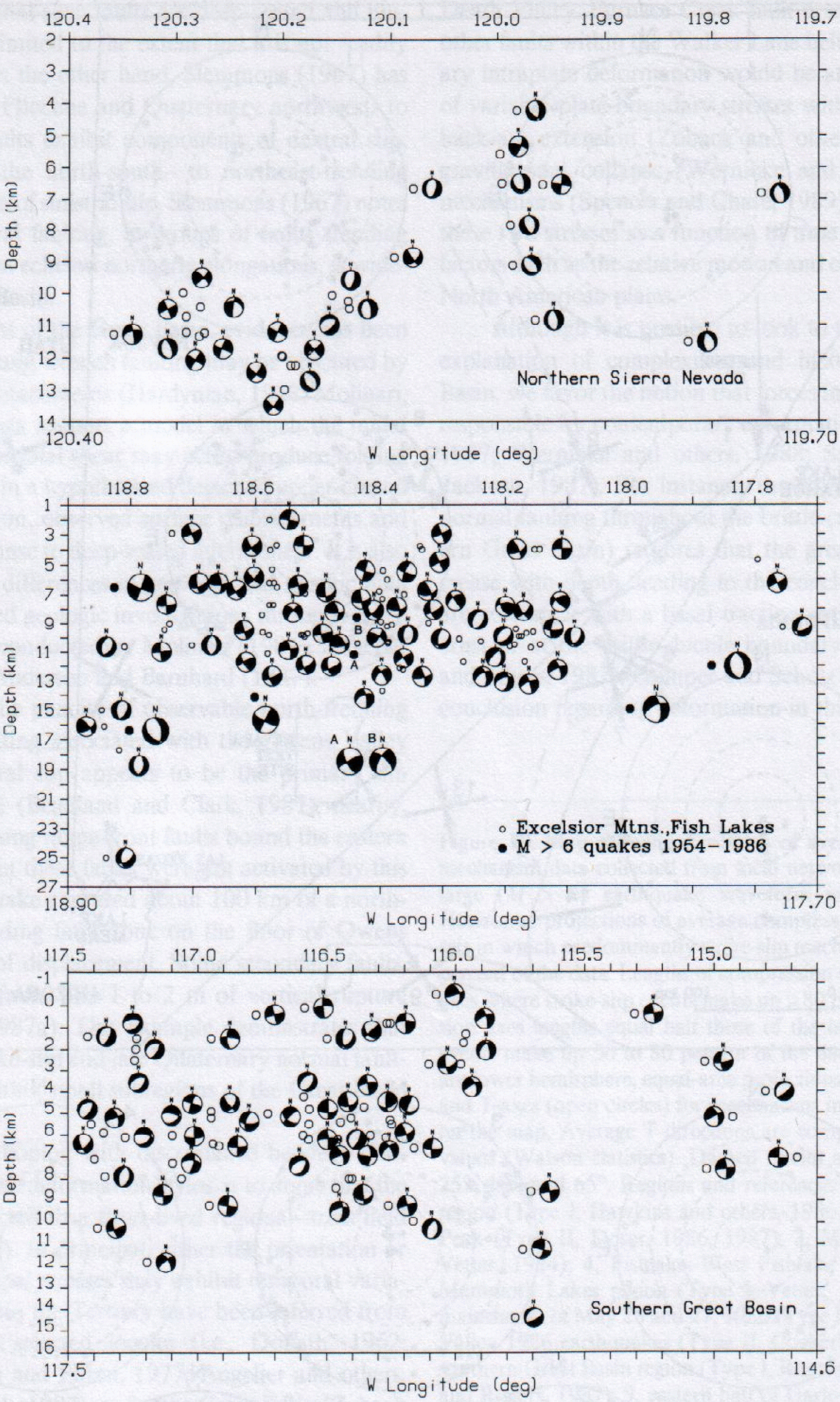

Figure 11. The east-west cross sections on which the focal mechanisms in Figures 6 and 7 have been projected. The focal hemispheres are lower hemisphere in plan view, shown at the focal depth. The larger focal spheres are events with M > 6. The solid dots labeled A and B are the locations of the events for focal mechanisms A and B. The events shown in the panels for the Northern Sierra region and the southern Great Basin are all less than magnitude 5.

of factors related to the temporal spread of volcanism, the location of the Nevada Seismic Zone, and crustal thickness between this zone and the eastern Sierra Nevada. Further, the slip direction for contemporary north-south strike slip is inconsistent with the slip direction that would be induced by remote plate-boundary influence (Atwater, 1970; Hill, 1982; Stewart, 1988), which could be taken as a contraindication for a plate-margin influence. Also, theoretical modeling of plate-boundary conditions by Sonder and others (1986) suggests that the Great Basin is too distant from the plate margin to be influenced significantly.

Some seismic (Doser, 1989; Arabasz and Julander, 1986) and geologic (Anderson and Barnhard, 1987) evidence exists for sinistral strike slip on northerly to northeasterly trending faults within the eastern Great Basin and possibly into the Colorado Plateau (Anderson and Christiansen, in preparation). On the basis of geologic and seismic data in the Sevier Valley, Utah, region, Anderson and Barnhard (1987) inferred locally active southerly transport of thin-skinned crustal blocks (upper 5 to 6 km). Mixtures of normal faulting and slip-incompatible strike-slip faulting suggest block-boundary faulting rather than a response to remote stress. This deformation style is more compatible with locally variable basal tractions than with regionally applied remote stresses.

Zoback (1989) noted that the orientation of the least-principal stress is roughly westerly along both the Colorado Plateau–Great Basin boundary and the Sierra Nevada–Basin and Range boundary, whereas within the interior Great Basin this stress is oriented northwest to N60°W. While it may be difficult to explain the origin of the geographic dependence in orientation of the least principal stress, it is equally difficult to explain the identical orientation of this stress at both province boundaries without inferring an internal deformation mechanism. A process wherein deformation interior to the Great Basin interacts with northerly trending province boundaries seems most plausible.

In a speculative vein, we suggest that the seismic data support a model of internally driven, southerly directed, lateral transport of the brittle crust in the southern Great Basin, a concept first proposed by Anderson (1984) on the basis of geologic data. Rogers and others (1987) suggested that the seismic data from the southern Great Basin were also best explained by this model. Given the data reviewed here, we suggest extension of this hypothesis to include the central Great Basin as well. Cartoons depicting this concept are shown in Figure 12. The existence of dextral motion on a series of subparallel faults across the central Great Basin and the presence of mixed mode and sinistral slip along the Colorado Plateau–Great Basin boundary suggest transport of a large subsection of the brittle crust in this region to the south. Oblique faulting may also occur as a secondary manifestation of the processes described by Hardyman (1978) and Molinari (1984) and is fundamentally related to deep-seated lateral slip. In this model, lateral deformation may extend through previously active shallow detachments in some locales, but not in all cases. In these areas, previously formed detachments may partially decouple deep-seated lateral shear from the surface. Normal and oblique faulting may also occur on north-northeasterly striking faults as pull-apart or right-offsets in essentially north-trending strike-slip zones (Figs. 12b). In this model the scarcity of easily detectable northerly trending lateral faults could be attributed to limited duration of the stresses driving this process and limited total slip. On the western margin of this zone, where the transported blocks abut the Walker Lane, the dextral motion could have been taken up along the northwest trends of that zone in the past, although this is not presently the pattern. Based on the Owens Valley event, southerly directed transport would extend to the Sierra Nevada boundary. On the eastern margin of the zone, where the blocks adjoin the Colorado Plateau, one would expect predominantly sinistral motion along north- to southeast-trending faults. These suggestions are highly speculative given the quantity of data available, the simplicity of this model, and its shortcomings. For example, the model implies that west-northwest extension is presently inactive, yet satellite geodesy data suggest that the Great Basin is extending 9.7 mm/yr in the direction N56°W (Minster and Jordan, 1987). The model also implies kinematic inconsistencies in some locales that could be expected to produce compressional features such as folding and reverse faulting. As yet, this style of deformation has not been observed in the seismic record.

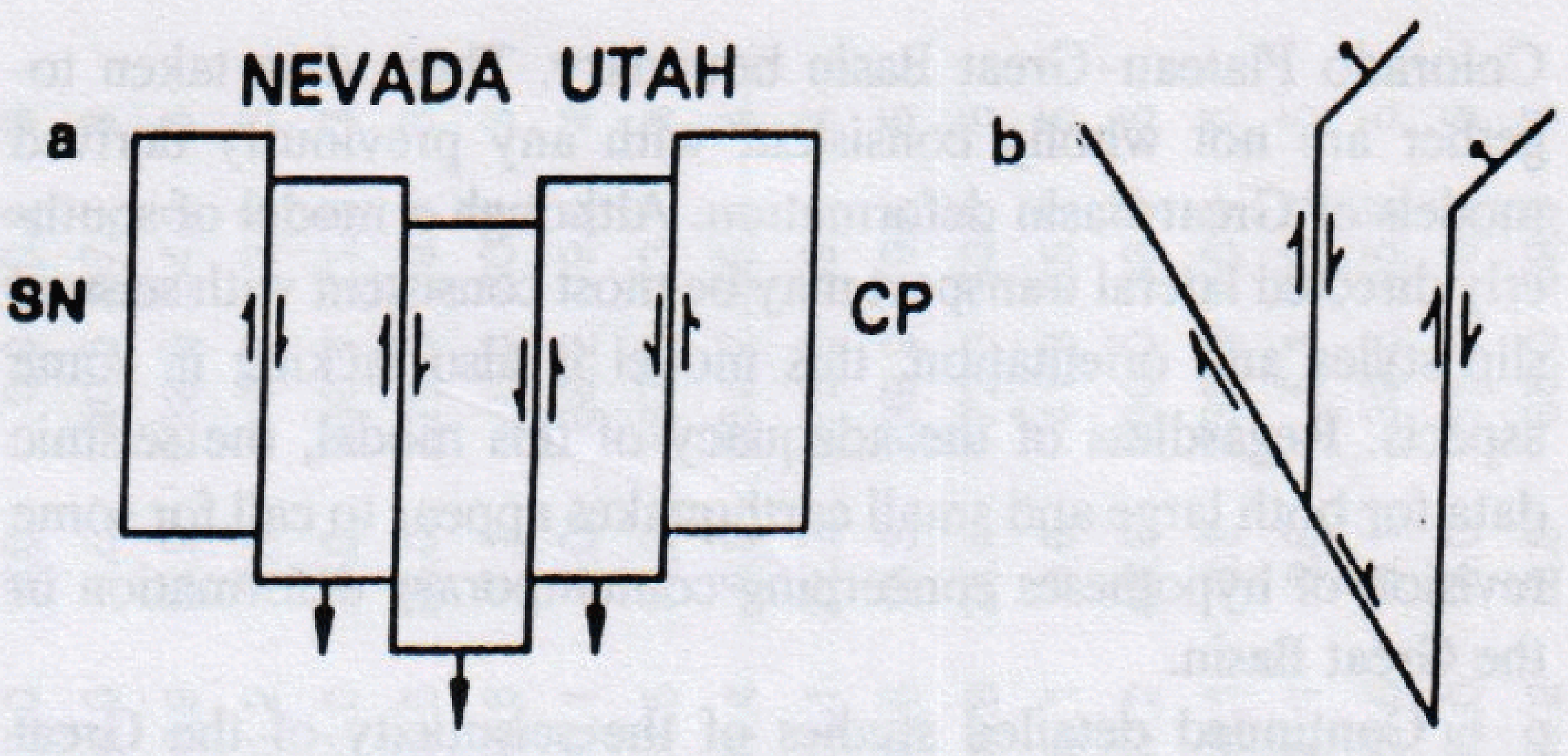

Figure 12. (a) Schematic diagram depicting dextral slip along north-trending faults in the southern (and possibly central) Great Basin, bounded by the Sierra Nevada block (SN), and sinistral slip along north-trending faults in the eastern margin of the Great Basin, bounded by the Colorado Plateau (CP). (b) Schematic diagram showing the relation between dextral slip on north-trending faults and normal slip on NNE-trending faults. The northwest-trending dextral slip fault could represent slip within the Walker Lane belt.

CONCLUSIONS

We find that seismic data from the Great Basin imply that substantial amounts of strike-slip and normal faulting are occurring at present. Furthermore, inconsistencies exist between the orientation and slip sense of faulting inferred from focal mechanisms and epicenter lineations compared with surface observations of historic fault rupture in the CNSB. Finally, although much of the inferred strike slip occurs as dextral slip on northerly trending faults, slip-incompatible dextral and sinistral slip has been noted on northerly to northeasterly trending faults near the

Colorado Plateau–Great Basin boundary. These data taken together are not wholly consistent with any previously derived models of Great Basin deformation. Although a model of southerly directed lateral transport may be most consistent with seismic slip styles and orientation, this model is also lacking in some aspects. Regardless of the adequacy of this model, the seismic data for both large and small earthquakes appear to call for some revision of hypotheses concerning contemporary deformation in the Great Basin.

Continued detailed studies of the seismicity of the Great Basin are required to help improve our understanding of deformation processes. For example, studies using high station densities centered in active zones would provide data to better define the geometry of active faults. Accurate estimates of earthquake depth are required to determine the vertical extent of strike-slip faulting; the relation between strike-slip faulting and multiple levels of normal and detachment faults that may exist within the crust is of primary importance for complete understanding of Great Basin deformation. Data from dense seismic networks would also permit more detailed study of the velocity structure of the upper crust, a factor that could act to constrain some deformation models. New geodetic data are also needed that span only the Great Basin and that are independent of deformation in other tectonic provinces. Although seismic data alone are not sufficient to resolve questions concerning Great Basin tectonics, continued collection of these and other kinds of geophysical and geologic data should help to further restrict the number of potential models.

TABLE A1. SELECTED GREAT BASIN FOCAL MECHANISMS 1972–1986

Origin time (UTC) Date	Time	North latitude	West longitude	Focal depth (km)	Mag	Region	Fig. 7 Index	Nodal plane Orientation St	Dp	Rk	Principal axes P Tr	P Pl	T Tr	T Pl	B Tr	B Pl	Ref.
1978 0209	03:47	34.884	-118.771	9.3	3.0	Garlock Fault Zone	1	150.0	44.0	139.0	27.1	10.7	133.6	56.2	290.4	31.6	1
1979 0517	00:37	35.069	-118.454	6.5	2.5	Garlock Fault Zone	2	118.0	74.0	90.0	208.0	29.0	28.0	61.0	118.0	0.0	1
1981 0612	02:59	35.069	-118.425	6.5	2.5	Garlock Fault Zone	3	154.0	80.0	-110.0	41.4	51.0	260.6	32.1	157.6	19.7	1
1977 1028	23:44	35.340	-117.917	8.1	2.5	Garlock Fault Zone	4	243.0	85.0	10.0	17.2	3.5	107.9	10.6	269.3	78.8	1
1980 0306	07:45	35.573	-117.237	5.2	2.5	Garlock Fault Zone	5	257.0	85.0	15.0	30.5	6.9	122.2	14.1	275.0	74.2	1
1978 0717	14:46	35.525	-116.236	3.2	2.5	Garlock Fault Zone	6	264.0	87.0	-53.0	206.2	36.9	324.0	31.8	81.7	36.9	1
1983 0703	15:08	39.415	-120.202	11.9	4.2	Truckee, California	7	26.0	90.0	0.0	161.0	0.0	71.0	0.0	0.0	90.0	2
1983 0703	12:48	39.424	-120.199	13.0	3.7	Truckee, California	8	38.0	80.0	-12.0	353.9	15.5	84.2	1.3	178.8	74.4	2
1981 0429	11:55	39.301	-119.754	6.8	4.2	Virginia City, Nevada	9	183.0	33.0	-68.0	214.9	71.8	77.2	13.6	344.3	11.8	2
1977 0201	18:47	39.091	-119.965	10.8	4.2	Lake Tahoe	10	180.0	34.0	-80.0	236.0	77.3	82.8	11.4	351.7	5.6	2
1981 0507	01:02	37.926	-118.524	9.8	4.6	Mono Lake	11	169.0	76.0	184.0	32.7	12.6	124.3	7.1	242.9	75.5	3
1981 0809	15.52	37.618	-118.920	8.2	3.7	Mammoth Lakes	12	10.0	80.0	-10.0	325.9	14.1	235.9	0.1	145.4	75.9	3
1981 0809	16:01	37.619	-118.919	14.2	4.3	Mammoth Lakes	13	0.0	75.0	-65.0	300.0	53.3	70.6	25.8	173.1	24.1	3
1982 0430	19:42	38.173	-118.334	14.2	3.0	Excelsior Mtns.	14	158.0	90.0	180.0	23.0	0.0	113.0	0.0	0.0	90.0	3
1982 0924	07:40	37.848	-118.159	10.7	5.3	Fishlake	15	66.0	100.0	20.0	201.4	21.2	294.0	6.6	40.5	67.7	3
1982 1228	19:06	37.990	-118.383	9.1	5.0	West Fishlake	16	66.0	78.0	-34.0	19.9	32.3	118.9	13.9	228.9	54.2	3
1982 1229	02:30	37.988	-118.387	10.3	2.5	West Fishlake	17	184.0	38.0	-86.0	251.7	82.5	91.2	7.1	0.8	2.5	3
1983 0101	01:32	38.070	-118.577	4.0	3.1	Mono Lake	18	147.0	75.0	191.0	10.0	18.3	101.0	3.0	200.1	71.5	3
1983 0106	11:09	37.984	-118.397	7.3	3.8	Fishlake	19	46.0	82.0	-50.0	352.0	39.4	105.6	26.0	219.3	39.5	3
1983 0117	23:20	37.936	-118.145	4.0	3.7	Fishlake	20	90.0	100.0	0.0	225.4	7.1	134.6	7.1	0.0	80.0	3
1979 0813	18:23	37.238	-115.029	7.6†	2.7	Pahranagat (SGB)	21	355.0	80.0	-177.0	219.3	9.2	310.1	5.0	68.2	79.6	4
1979 1225	14:17	37.288	-117.062	8.0†	2.8	Sarcobatus Flat (SGB)	22	88.0	74.0	3.0	43.7	9.2	311.5	13.3	167.2	73.7	4
1982 0706	02:10	37.698	-115.037	2.6†	3.2	Hancock Summit (SGB)	23	177.5	69.0	-167.0	38.7	23.7	131.4	6.0	234.7	65.5	4
1983 0102	16:32	36.502	-116.569	5.5†	2.6	Rock Valley (SGB)	24	9.1	60.0	3.0	49.2	18.8	311.1	22.7	175.0	59.9	4
1985 0113	22:21	36.366	-115.769	14.4†	2.5	Mt. Sterling (SGB)	25	221.0	27.0	249.0	354.5	68.4	146.6	19.3	239.9	9.4	5
1985 0120	18:40	36.617	-116.444	5.4†	2.3	Lathrop Wells (SGB)	26	75.5	50.2	-4.2	39.6	29.5	294.8	24.4	172.0	50.0	5
1985 0515	10:29	37.455	-115.309	0.5†	2.3	Hancock Summit (SGB)	27	260.0	87.0	-3.8	215.1	4.8	305.1	0.6	41.8	85.2	5
1985 0530	05:46	37.113	-116.262	5.5†	1.7	Nevada Test Site (SGB)	28	177.4	74.4	50.3	296.0	19.5	47.2	45.6	190.0	38.0	5
1985 1212	11:57	36.860	-116.726	5.0†	1.5	Bare Mountain (SGB)	29	92.7	65.6	-32.7	53.5	39.8	146.1	3.2	239.9	50.0	5
1986 0116	15:24	36.873	-115.984	1.7†	2.0	Nevada Test Site (SGB)	30	220.5	44.8	315.0	204.5	58.7	100.1	8.6	5.1	29.9	5
1986 0217	20:29	37.020	-116.464	8.4†	1.5	Timber Mountain (SGB)	31	255.0	60.0	325.0	219.7	44.8	129.6	0.1	39.5	45.2	5
1986 0306	20:16	37.160	-117.359	8.0†	2.6	Ubehebe Crater (SGB)	32	15.0	40.0	270.0	105.0	85.0	285.0	5.0	15.0	0.0	5
1986 0306	20:29	37.158	-117.366	6.0†	1.8	Ubehebe Crater (SGB)	33	341.0	60.0	183.0	201.1	22.7	299.2	18.8	65.0	59.9	5

TABLE A1. GREAT BASIN FOCAL MECHANISMS 1972–1986 (continued)

Origin time (UTC) Date	Time	North latitude	West longitude	Focal depth (km)	Mag	Region	Fig. 7 Index	Nodal plane Orientation St	Dp	Rk	Principal axes P Tr	P Pl	T Tr	T Pl	B Tr	B Pl	Ref.
1986 0604	15:07	37.345	-117.236	1.5†	2.8	Scottys Junction (SGB)	34	266.0	52.8	-64.6	235.7	69.4	338.3	4.7	70.0	20.0	5
1986 0702	08:10	36.599	-116.407	5.2†	2.6	Lathrop Wells (SGB)	35	244.1	85.8	-24.7	197.3	20.3	292.6	14.1	55.1	65.0	5
1986 1206	09:20	36.462	-116.165	9.9†	2.5	Amargosa Flat (SGB)	36	206.9	55.6	-77.9	154.4	75.9	288.2	9.8	20.0	10.0	5
1977 1231	03:43	38.899	-117.984	12.4	3.1	CNSB	37	31.0	40.0	-85.0	85.1	84.0	297.5	5.1	207.2	3.2	3
1978 0215	09:25	39.552	-118.442	12.0	4.0	CNSB	38	64.0	40.0	-48.0	57.7	61.6	305.1	11.8	209.4	25.5	3
1980 0926	06:07	39.471	-118.133	11.8	3.2	CNSB	39	66.0	62.0	-132.0	284.6	52.7	184.5	7.6	88.9	36.2	3
1986 0708	03:02	36.645	-117.195	11.8†	2.4	Death Valley (SGB)	40	232.0	77.8	-27.6	187.2	28.0	282.5	9.8	30.0	60.0	5
1972 1020	23:16	36.093	-114.678	6.2	1.6	Lake Mead (SGB)	41	94.0	89.9	0.0	49.0	0.1	319.0	0.1	184.0	89.9	6
1972 1209	06:46	36.042	-114.802	3.1	2.6	Lake Mead (SGB)	42	52.0	70.0	-90.0	322.0	65.0	142.0	25.0	52.0	0.0	6

Notes: This table presents the data for selected focal mechanisms shown in Figure 7 for earthquakes recorded by various Great Basin seismograph networks. The mechanisms are based on P-wave first-motion studies. Focal depth is relative to the surface except where a dagger (†) follows the depth estimate, in which case depth is relative to sea level or 0 km. Magnitude (Mag), indicating the size of the earthquake, is ML (local) or MD (duration). The symbols are: St = strike of nodal plane, Rk = rake of slip vector; principal axes are pressure (P), tension (T), and null (B); Tr = trend of axis, Pl = plunge of axis. No inferred fault planes for these focal mechanisms are suggested in this table; however, only one of the two nodal planes is indicated above. References: 1. Astiz and Allen (1983); 2. Hawkins and others (1986); 3. Vetter and Ryall (1983); 4. Rogers and others (1987); 5. Harmsen and Rogers (1987); 6. Rogers and Lee (1976). (SGB) = earthquakes in the Southern Great Basin.

TABLE A2. SELECTED FOCAL MECHANISMS FROM THE LARGEST GREAT BASIN EARTHQUAKES

Origin time (UTC) Date	Time	North latitude	West longitude	Focal depth (km)	Mag (ML)	Fig 6 Index	Nodal plane Orientation St	Dp	Rk	Principal axes P Tr	P Pl	T Tr	T Pl	B Tr	B Pl	Ref.
1932 1221	6:10a	38.68	-118.21	14	7.2	1	1.0	72.0	-176.0	224.0	15.4	316.7	9.9	78.2	71.6	2
1932 1221	6:10b	38.46	-117.97	12	6.2	2	347.0	81.0	-179.0	211.6	7.1	302.3	5.6	70.6	80.9	2
1934 0130	20:16	38.26	-118.46	14	6.3	3	248.0	40.0	-91.0	346.1	85.0	158.7	5.0	248.8	0.6	2
1934 0312	15:05	41.658	-112.795	9	6.6	4	42.0	90.0	-12.0	356.4	8.5	87.6	8.5	222.0	78.0	3
1934 0312	18:20	41.571	-112.745	8	6.1	5	25.0	85.0	-29.0	337.5	23.8	74.9	16.3	196.1	60.6	3
1954 0706	11:13	39.29	-118.36	10	6.8	6	336.0	78.0	-140.0	203.8	36.3	100.6	17.3	349.9	48.5	1
1954 0706	22:07	39.20	-118.40	8	6.4	7	348.0	70.0	-157.0	209.2	30.1	118.6	1.0	26.9	59.9	1
1954 0824	05:51	39.35	-118.34	12	6.8	8	355.0	50.0	-145.0	200.9	49.9	300.8	8.3	37.6	38.9	1
1954 0831	22:20	39.72	-118.47		5.8	9	22.0	55.0	-160.0	235.5	37.1	334.8	12.0	79.6	50.3	1
1954 0901	05:18	39.70	-118.40		5.5	10	20.0	70.0	-42.0	336.3	43.4	77.5	11.7	179.2	44.3	1
1954 1216	11:07	39.20	-118.00	15	7.3	11	350.0	60.0	-160.0	206.5	34.3	302.2	8.3	43.9	54.5	1
1954 1216	11:11	39.67	-117.87	12	6.9	12	350.0	50.0	-90.0	260.0	85.0	80.0	5.0	170.0	0.0	1
1959 0323	07:10	39.43	-117.99		6.3	13	2.0	45.0	178.0	218.2	28.9	327.7	31.2	94.8	45.0	1
1959 0623	14:35	38.92	-118.89		6.3	14	310.0	68.0	-138.0	172.3	44.7	72.2	10.0	332.6	43.6	1
1966 0816	18:02	37.395	-114.206	7.0	6.0	15	17.0	80.0	190.0	241.1	14.1	331.1	0.1	61.6	75.9	4
1980 0525	16.33	37.589	-118.826	6.5	6.5	16	21.0	87.0	-6.0	336.0	6.4	66.3	2.1	174.5	83.3	5
1980 0527	14:50	37.470	-118.802	16.4	6.3	17	135.0	42.0	-118.0	316.6	70.6	64.5	6.2	156.6	18.3	5
1984 0112	03:18	37.456	-118.602	14.1	6.2	18	207.7	86.5	10.2	342.0	4.7	72.8	9.7	226.4	79.2	6
1986 0720	14:29	37.540	-118.439	8.6	6.2	19	205.0	75.0	-20.0	171.2	34.7	80.1	1.6	347.8	55.2	7
1986 0721	14:42	37.540	-118.442	11.2	6.6	20	155.0	60.0	-180.0	14.1	10.3	107.7	19.0	257.2	68.2	7

Notes: This table presents the data for the selected focal mechanisms shown in Figure 6 for Great Basin earthquakes having magnitude $\geq$5.5. These machanisms were computed using waveform inversion techniques (except events 19 and 20, which are computed from P-wave first-motion polarities). St = strike of nodal plane, Dp = dip of nodal plane, Rk = rake of slip vector; principal axes are Pressure (p), Tension (T), and Null (B); Tr = trend of axis, Pl = plunge of axis; Mag = local magnitude. Nodal planes: no inferred fault planes for these focal mechanisms are suggested in this table; however, only one of the two nodal planes is indicated above.Ref = references: 1. Doser (1986); 2. Doser (1988); 3. Doser (1989); 4. Smith and Lindh (1978); 5. Sipkin (1986); 6. Barker and Wallace (1986); 7. Cockerham and Corbett (1987).

REFERENCES CITED

Aki, K., and Tsai, Y., 1972, Mechanism of Love-wave excitation by explosive sources: Journal of Geophysical Research, v. 77, p. 1452–1475.

Aki, K., Reasenberg, P., DeFazio, T., and Tsai, Y., 1969, Near-field and far-field seismic evidences for triggering of an earthquake by the Benham explosion: Seismological Society of America Bulletin, v. 59, no. 6, p. 2197–2207.

Algermissen, S. T., Perkins, D. M., Thenhaus, P. C., Hanson, S. L., and Bender, B. L., 1982, Probabilistic estimates of maximum acceleration and velocity in rock in the contiguous United States: U.S. Geological Survey Open-File Report 82-1033, 99 p.

Anderson, D. L., 1971, The San Andreas fault: Scientific America, v. 225, p. 52–67.

Anderson, L. W., and Hawkins, F. F., 1984, Recurrent Holocene strike-slip faulting, Pyramid Lake fault zone, western Nevada: Geology, v. 12, p. 681–684.

Anderson, R. E., 1971, Thin-skinned distension in Tertiary rocks of southeastern Nevada: Geological Society of America Bulletin, v. 82, p. 43–58.

——, 1973, Large magnitude late Tertiary strike-slip faulting north of Lake Mead, Nevada: U.S. Geological Survey Professional Paper 794, 18 p.

——, 1984, Strike-slip faults associated with extension in and adjacent to the Great Basin: Geological Society of America Abstracts with Programs, v. 16, p. 429.

Anderson, R. E., and Barnhard, T. P., 1987, Neotectonic framework of the central Sevier Valley area, Utah, and its relationship to seismicity, *in* Gori, P. L., and Hays, W. W., eds., Assessment of regional hazards and risk along the Wasatch Front, Utah: U.S. Geological Survey Open-File Report 87-585, p. F1–134.

Anderson, R. E., and Ekren, E. B., 1977, Late Cenozoic fault patterns and stress fields in the Great Basin and westward displacement of the Sierra Nevada block: Geology, v. 5, p. 388–389.

Anderson, R. E., Zoback, M. L., and Thompson, G. A., 1983, Implications of selected subsurface data on the structural forms and evolution of some basins in the northern Basin and Range Province, Nevada and Utah: Geological Society of America Bulletin, v. 94, p. 1055–1072.

Angelier, J., Colletta, B., and Anderson, R. E., 1985, Neocene paleostress changes in the Basin and Range; A case study of Hoover Dam, Nevada-Arizona: Geological Society of America Bulletin, v. 96, p. 347–361.

Arabasz, W. J., and Julander, D. R., 1986, Geometry of seismically active faults and crustal deformation within the Basin and Range–Colorado Plateau transition in Utah, *in* Mayer, L., ed., Extensional tectonics of the southwestern United States; A perspective on processes and kinematics: Geological Society of American Special Paper 208, p. 43–74.

Astiz, L., and Allen, C. R., 1983, Seismicity of the Garlock fault, California: Seismological Society of America Bulletin, v. 73, p. 1721–1734.

Atwater, T., 1970, Implications of plate tectonics for the Cenozoic tectonic evolution of western North America: Geological Society of America Bulletin, v. 81, p. 3513–3536.

Baker, M. R., and Doser, D. I., 1988, Joint inversion of regional and teleseismic waveforms: Journal of Geophysical Research, v. 93, p. 2037–2045.

Barker, J. S., and Wallace, T. C., 1986, A note on the teleseismic body waves for the 23 November 1984 Round Valley, California, earthquake: Seismological Society of America Bulletin, v. 76, p. 883–888.

Bateman, P. C., 1961, Willard D. Johnson and the strike-slip component of fault movement in the Owens Valley, California, earthquake of 1872: Seismological Society of America Bulletin, v. 51, no. 4, p. 483–493.

Beanland, S., and Clark, M. M., 1987, The Owens Valley fault zone, eastern California, and surface rupture associated with the 1872 earthquake: Seismological Resarch Letters, v. 58, p. 32.

Beck, P. J., 1970, The southern Nevada–Utah border earthquakes, August to December, 1966 [M.S. thesis]: Salt Lake City, University of Utah, 62 p.

Bender, B., 1983, Maximum likelihood estimation of b values for magnitude grouped data: Seismological Society of America Bulletin, v. 73, p. 831–851.

Boucher, G., Seeber, L., Ward, P., and Oliver, J., 1967, Microaftershock observations at the epicenter of a moderate-sized earthquake in Nevada: EOS Transactions of the American Geophysical Union, v. 48, p. 205.

Boucher, G., Ryall, N., and Jones, A. E., 1969, Earthquakes associated with underground nuclear explosions: Journal of Geophysical Research, v. 74, p. 3809–3820.

Bucknam, R. C., 1969, Geologic effects of the Benham underground nuclear explosion, Nevada Test Site: Seismological Society of America Bulletin, v. 59, p. 2209–2220.

Bucknam, R. C., Algermissen, S. T., and Anderson, R. E., 1980, Patterns of late Quaternary faulting in western Utah and an application in earthquake hazard evaluation, *in* Anderson, R. E., Ryall, A., and Smith, R. A., eds., Earthquake hazards along the Wasatch and Sierra-Nevada frontal fault zones: U.S. Geological Survey Open-File Report 80-801, p. 299–314.

Byerly, P., and 5 others, 1956, The Fallon-Stillwater earthquakes of July 6, 1954, and August 23, 1954: Seismological Society of America Bulletin, v. 46, p. 1–40.

Callaghan, E., and Gianella, V., 1935, The earthquake of January 30, 1934, at Excelsior Mountains, Nevada: Seismological Society of America Bulletin, v. 47, p. 327–334.

Cloud, W. K., 1957, Intensity distribution and strong-motion seismograph results, Nevada earthquakes of December 16, 1954: Seismological Society of America Bulletin, v. 47, p. 327–334.

Cockerham, R. S., and Corbett, E. J., 1987, The July 1986 Chalfant Valley, California, earthquake sequence; Preliminary results: Seismological Society of America Bulletin, v. 77, p. 280–289.

Coffman, J. L., and von Hake, C. A., 1973, Earthquake history of the United States: U.S. Department of Commerce, National Oceanic and Atmospheric Administration NOAA EDS Publication 41-1/COM 74 500 35, 108 p.

Coney, D. J., and Harms, T. A., 1984, Cordilleran metamorphic core complexes; Cenozoic extensional relics of Mesozoic compression: Geology, v. 12, p. 550–554.

Coney, P. J., 1987, The regional tectonic setting and possible causes of Cenozoic extension in the North American Cordillera, *in* Coward, M., and others, eds., Continental extensional tectonics: Geological Society of London Special Publication 28, p. 177–186.

dePolo, C. M., and Ramelli, A. R., 1987, Preliminary report on surface fractures along the White Mountains fault zone associated with the July 1986 Chalfant Valley earthquake sequence: Seismological Society of America Bulletin, v. 77, p. 290–296.

dePolo, C. M., Bell, J. W., and Ramelli, A. R., 1987, Geometry of strike-slip faulting related to the 1932 Cedar Mountain earthquake, central Nevada: Geological Society of America Abstracts with Programs, v. 19, p. 371.

Dewey, J. W., and Spence, W., 1979, Seismic gaps and source zones of recent large earthquakes in coastal Peru: Pure and Applied Geophysics, v. 117, p. 1148–1171.

Donath, F. A., 1962, Analyses of basin-range structure, south-central Oregon: Geological Society of America Bulletin, v. 73, p. 1–16.

Doser, D. I., 1986, Earthquake processes in the Rainbow Mountain–Fairview Peak–Dixie Valley, Nevada, region (1954–1959): Journal of Geophysical Research, v. 91, p. 12572–12586.

——, 1987, Modeling Pnl waveforms of the Fairview Peak–Dixie Valley, Nevada, U.S.A., earthquake sequence (1954–1959): Physics of the Earth and Planetary Interiors, v. 48, p. 64–72.

——, 1988, Source mechanisms of earthquakes in the Nevada seismic zone (1915–1943) and implications for deformation in the western Great Basin: Journal of Geophysical Research, v. 93, p. 15001–15015.

——, 1989, Extensional tectonics in northern Utah, U.S.A.; The 1934 Hansel Valley sequence: Physics of the Earth and Planetary Interiors, v. 54, p. 120–143.

Doser, D. I., and Smith, R. B., 1985, Source parameters of the 28 October 1983, Borah Peak, Idaho, earthquake from body wave analysis: Seismological Society of America Bulletin, v. 75, p. 1041–1051.

Douglas, B. M., and Ryall, A., 1972, Special characteristics and stress drop for microearthquakes near Fairview Peak, Nevada: Journal of Geophysical Research, v. 77, p. 351–359.

Eaton, G. P., Wahl, R. R., Prostka, H. J., Mabey, D. R., and Kleinkopf, M. D., 1978, Regional gravity and tectonic patterns; Their relation to late Cenozoic epeirogeny and lateral spreading in the western Cordillera, *in* Smith, R. B., and Eaton, G. P., eds., Cenozoic tectonics and regional geophysics of the western Cordillera: Geological Society of America Memoir 152, p. 51–91.

Eddington, P. K., Smith, R. B., and Renggli, C., 1987, Kinematics of Basin and Range intraplate extension, *in* Coward, M., and others, eds., Continental extensional tectonics: Geological Society of London Special Publication 28, p. 371–392.

Fara, H. D., 1964, A new catalog of earthquake fault plane solutions: Seismological Society of America Bulletin, v. 54, p. 1491–1518.

Fischer, F. G., Papanek, P. J., and Hamilton, R. M., 1972, The Massachusetts Mountain earthquake of 5 August 1971 and its aftershocks, Nevada Test Site: U.S. Geological Survey Report USGS-474-149; available only from U.S. Department of Commerce National Technical Information Service, Springfield, Virginia 22161 as Report NTS-238, 20 p.

Frizzell, V. A., and Zoback, M. L., 1987, Stress orientation determined from fault slip data in Hampel Wash area, Nevada, and its relation to contemporary regional stress field: Tectonics, v. 6, p. 89–98.

Gawthrop, H. W., and Carr, W. J., 1988, Location refinement of earthquakes in the southwestern Great Basin, 1931–1974, and seismotectonic characteristics of some of the important events: U.S. Geological Survey Open-File Report 88-560, 64 p.

Gianella, V. P., and Callaghan, E., 1934a, The earthquake of December 20, 1932, at Cedar Mountain, Nevada, and its bearing on the genesis of Basin-Range structure: Journal of Geology, v. 42, p. 1–22.

——, 1934b, The Cedar Mountains, Nevada, earthquake of December 20, 1932: Seismological Society of America Bulletin, v. 24, p. 345–384.

Gross, W. K., and Savage, J. C., 1987, Deformation associated with the 1986 Chalfant Valley earthquake, eastern California: Seismological Society of America Bulletin, v. 77, p. 306–310.

Gumper, F. J., and Scholz, C., 1971, Microseismicity of the Nevada seismic zone: Seismological Society of America Bulletin, v. 61, p. 1413–1432.

Hamilton, R. M., and Healy, J. H., 1969, Aftershocks of the Benham nuclear explosion: Seismological Society of America Bulletin, v. 59, p. 2271–2281.

Hamilton, R. M., Smith, B. E., Fischer, F. G., and Papanek, P. J., 1971, Seismicity of the Pahute Mesa area, Nevada Test Site, 8 December 1968 through 31 December 1971: U.S. Geological Survey Report USGS-474-138, 170 p; available only from U.S. Department of Commerce, National Technical Information Service, Springfield, Virginia 22161.

Hamilton, W., and Myers, W. B., 1966, Cenozoic tectonics of the western United States: Review of Geophysics, v. 4, p. 509–549.

Hanks, T. C., and Kanamori, H., 1979, A moment magnitude scale: Journal of Geophysical Research, v. 84, p. 2348–2350.

Hardyman, R. F.,1978, Volcanic stratigraphy and structural geology of Gillis Canyon Quadrangle, northern Gillis Range, Mineral County, Nevada [Ph.D. thesis]: Reno University of Nevada, 248 p.

Harmsen, S. C., and Rogers, A. M., 1986, Inferences above the local stress field from focal mechanisms; Applications to earthquakes in the southern Great Basin of Nevada: Seismological Society of America, v. 76, p. 1560–1572.

——, 1987, Earthquake location data for the southern Great Basin of Nevada and California; 1984 through 1986: U.S. Geological Survey Open-File Report 87-596, 92 p.

Hawkins, F. F., LaForge, R., and Hansen, R. A., 1986, Seismotectonic study of the Truckee/Lake Tahoe area, northeastern Sierra Nevada, California, for Stampede, Prosser Creek, Boca, and Lake Tahoe dams: U.S. Bureau of Reclamation Seismotectonic Report 85-4, 210 p.

Hill, D. P., 1982, Contemporary block tectonics; California and Nevada: Journal of Geophysical Research, v. 87, p. 5433–5450.

Hill, D. P., Wallace, R. E., and Cockerham, R. S., 1985, A review of evidence on the potential for major earthquakes and volcanism in the Long Valley–Mono Craters–White Mountains region of eastern California: Earthquake Prediction Research, v. 3, p. 571–594.

Holden, E. S., 1898, Catalogue of earthquakes on the Pacific coast 1769 to 1897: Smithsonian Institute Miscellaneous Collections, no. 1087, 253 p.

Hunt, C. B., and Mabey, D. R., 1966, General geology of Death Valley, California; Stratigraphy and structure: U.S. Geological Survey Professional Paper 494-A, p. A1–A165.

Jackson, J. A., 1987, Active normal faulting and crustal extension, *in* Coward, M., and others, eds., Continental extensional tectonics: Geological Society of London Special Publication 28, p. 3–17.

Jones, A. E., 1963, Catalog of Nevada earthquakes; Part 2, Study of Wiechert records at Reno, 1916–1950: Geological Society of America Special Paper 76, 206 p.

——, 1975, Recording of earthquakes at Reno, 1916–1951, *in* Van Wormer, J. D., ed., Bulletin of the Seismological Laboratory: Reno, University of Nevada Seismological Laboratory Report, 199 p.

Jones, J. C., 1915, The Pleasant Valley, Nevada, earthquake of October 2, 1915: Seismological Society of America Bulletin, v. 5, p. 190–205.

Jones, L. M., and Dollar, R. S., 1986, Evidence of Basin-and-Range extensional tectonics in the Sierra Nevada; The Durrwood Meadows swarm, Tulare County, California (1983–1984): Seismological Society of America Bulletin, v. 76, p. 439–461.

Lay, T., Wallace, T. C., and Helmberger, D. V., 1984, The effects of tectonic release on short-period P-waves from NTS explosions: Seismological Society of America Bulletin, v. 74, p. 819–842.

Lubetkin, K. C., and Clark, M. M., 1987a, Late Quaternary activity along the Lone Pine fault, eastern California: Seismological Research Letters, v. 58, p. 32.

——, 1987b, Late Quaternary fault scarp at Lone Pine, California; Location of oblique slip during the great 1872 earthquake and earlier earthquakes, *in* Hill, M. L., ed., Cordilleran Section of the Geological Society of America: Boulder, Colorado, Geological Society of America Centennial Field Guide 1, p. 151–156.

Maldonado, F., 1977a, Results from fault-monitoring stations on Pahute Mesa, Nevada Test Site, from July 1973 through December 1976: U.S. Geological Survey Report USGS-474-242, 32 p.; available only from U.S. Department of Commerce National Technical Information Service, Springfield, Virginia 22161.

——, Composite postshot fracture map of Pahute Mesa, Nevada Test Site, June 1973 through March 1976: U.S. Geological Survey Report USGS-474-243, 8 p.; available only from U.S. Department of Commerce National Technical Information Service, Springfield, Virginia 22161.

Mark, R. K., 1977, Application of linear statistical models of earthquake magnitude versus fault length in estimating maximum expectable magnitude earthquakes: Geology, v. 5, p. 464–466.

Matthews, V., III, and Anderson, C. E., 1973, Yellowstone convection plume and break-up of the western United States: Nature, v. 243, p. 158–159.

McAdie, A. G., 1907, Catalog of earthquakes on the Pacific coast 1897–1906: Smithsonian Institute Miscellaneous Collections, no. 1721, 64 p.

McGarr, A., 1982, Analysis of states of stress between provinces of constant stress: Journal of Geophysical Research, v. 87, p. 9279–9288.

McKeown, F. A., 1975, Relation of geological structure to seismicity at Pahute Mesa, Nevada Test Site: Seismological Society of America Bulletin, v. 65, p. 747–764.

McKeown, F. A., and Dickey, D. D., 1969, Fault displacements and motion related to nuclear explosions: Seismological Society of America Bulletin, v. 59, no. 6, p. 2253–2269.

Mead, T. C., and Carder, D. S., 1941, Seismic investigation in the Boulder Dam area in 1939: Seismological Society of America Bulletin, v. 31, p. 321–324.

Meister, L. J., Burford, R. O., Thompson, G. A., and Kovach, R. L., 1968, Surface strain changes and strain energy release in the Dixie Valley-Fairview Peak area, Nevada: Journal of Geophysical Research, v. 73, p. 5981–5994.

Meremonte, M. E., and Rogers, A. M., 1987, Historical catalog of southern Great Basin earthquakes 1868–1978, U.S. Geological Survey Open-File Report 87-80, 203 p.

Miller, C. D., Crandell, D. R., Mullineaux, D. R., Hoblitt, R. P., and Bailey, R. A., 1982, Preliminary assessment of potential volcanic hazards in the Long Valley–Mono Lakes area, east-central California and southwestern Nevada: U.S. Geological Survey Open-File Report 82-583, 30 p.

Minster, J. B., and Jordan, T. H., 1987, Vector constraints on western U.S. deformation from space geodesy: Neotectonics and plate motion: Journal of Geophysical Research, v. 92, p. 4798–4804.

Molinari, M. P., 1984, Late Cenozoic geology and tectonics of Stewart and Monte Cristo valleys, west-central Nevada [M.S. thesis]: Reno, University of Nevada, 124 p.

Morris, R. H., 1971, Geologic effects, *in* Geologic and hydrologic effects of the Handley event, Pahute Mesa, Nevada Test Site: U.S. Geological Survey Report USGS-474-95, p. 7–26; available only from U.S. Department of Commerce National Technical Information Service, Springfield, Virginia 22161.

Nakata, J. K., Wentworth, C. M., and Machette, M. N., 1982, Quaternary fault map of the Basin and Range and Rio Grande Rift Provinces, western United States: U.S. Geological Survey Open-File Report 82-579, scale 1:2,500,000.

Oakeshott, G. B., Greensfelder, R. W., and Kahle, J. E., 1972, The Owens Valley earthquake of 1872; One hundred years later: California Geology, v. 25, p. 55–62.

Okaya, D. A., and Thompson, G. A., 1985, Geometry of Cenozoic extensional faulting; Dixie Valley, Nevada: Tectonics, v. 4, no. 1, p. 107–125.

Oliver, J., Ryall, A. Brune, J. N., and Slemmons, D. B., 1966, Microearthquake activity recorded by portable seismographs of high sensitivity: Seismological Society of America Bulletin, v. 56, p. 899–924.

Orkild, P. P., Sargent, K. A., and Snyder, R. P., 1969, Geologic map of Pahute Mesa, Nevada Test Site and vicinity, Nye County, Nevada: U.S. Geological Survey Miscellaneous Geologic Investigations Map I-567, scale 1:48,000.

Pacheco, J., and Nábělek, J., 1988, Source mechanisms of three moderate California earthquakes of July 1986, Seismological Society of America Bulletin, v. 78, no. 6, p. 1907–1929.

Page, B. M., 1935, Basin-Range faulting of 1915 in Pleasant Valley, Nevada: Journal of Geology, v. 43, p. 690–707.

Page, R., 1968, Focal depths of aftershocks: Journal of Geophysical Reseerch, v. 713, p. 3897–3903.

Papanek, P. J., and Hamilton, R. M., 1972, A seismicity study along the northern Death Valley–Furnace Creek fault zone, California-Nevada boundary: U.S. Geological Survey Report USGS-474-141, 41 p.; available only from U.S. Department of Commerce National Technical Information Service, Springfield, Virginia 22161.

Perkins, D. M., 1987, Contiguous fault rupture, probabilistic hazard, and contagion observability, *in* Crone, A. J., and Omdahl, E. M., eds., Directions in paleoseismology; Proceedings of Conference 39: U.S. Geological Survey Open-File Report 87-673, p. 428–439.

Real, C. R., Toppozada, T. R., and Parke, D. L., 1978, Earthquake epicenter map of California showing events from 1900 through 1974 equal to or greater than magnitude 4.0 or intensity V: California Division of Mines and Geology Map Sheet 39, scale 1:1,000,000.

Richins, W. D., and 5 others, 1985, The 1983 Borah Peak, Idaho, earthquake; Relationship of aftershocks to the mainshock, surface faulting, and regional tectonics, *in* Stein, R. S., and Bucknam, R. C., eds., Proceedings of Workshop 28 on the Borah Peak, Idaho, earthquake: U.S. Geological Survey Open-File Report 85-290A, p. 285–310.

Richter, C. F., 1958, Elementary seismology: San Francisco, California, W. H. Freeman, 768 p.

Rogers, A. M., and Lee, W.H.K., 1976, Seismic study of earthquakes in the Lake Mead, Nevada-Arizona region: Seismological Society of America Bulletin, v. 66, no. 5, p. 1657–1681.

Rogers, A. M., Woulett, G. M., and Covington, P. A., 1977, Seismicity of the Pahute Mesa area, Nevada Test Site, 8 October 1975 to 30 June 1976: U.S. Geological Survey Report USGS-474-184; available only from U.S. Department of Commerce National Technical Information Service, Springfield, Virginia 22161.

Rogers, A. M., Harmsen, S. C., Carr, W. J., and Spence, W. J., 1983, Southern Great Basin seismological data report for 1981 and preliminary data analysis: U.S. Geological Survey Open-File Report 83-669, 240 p.

Rogers, A. M., Harmsen, S. C., and Meremonte, M. E., 1987, Evaluation of the seismicity of the southern Great Basin and its relationship to the tectonic framework of the region: U.S. Geological Survey Open-File Report 87-408, 196 p.

Romney, C. F., 1957, The Dixie Valley–Fairview Peak, Nevada, earthquakes of December 16, 1954; Seismic waves: Seismological Society of America Bulletin, v. 47, p. 301–320.

Ron, H., Aydin, A., and Nur, A., 1986, The role of strike-slip faulting in the deformation of Basin and Range provinces [abs.]: EOS Transactions of the American Geophysical Union, v. 67, p. 358.

Ryall, A. S., 1977, Earthquake hazard in the Nevada region: Seismological Society of America Bulletin, v. 67, p. 517–532.

Ryall, A. S., and Douglas, B. M., 1974, Seismicity of northwest Nevada related to the feasibility of power plant siting: Reno, Nevada, Report to Sierra Pacific Power Company, 79 p.

Ryall, A. S., and Malone, S. D., 1971, Earthquake distribution and mechanism of faulting in the Rainbow Mountain–Dixie Valley–Fairview Peak area, central Nevada: Journal of Geophysical Research, v. 76, p. 7241–7248.

Ryall, A. S., and Priestly, K., 1975, Seismicity, secular strain, and maximum magnitude in the Excelsior Mountain area, western Nevada and eastern California: Geological Society of America Bulletin, v. 86, p. 1585–1592.

Ryall, A. S., and Ryall, F., 1981, Spatial-temporal variations in seismicity preceding the May 1980 Mammoth Lakes earthquakes, California: Seismological Society of America Bulletin, v. 71, p. 747–760.

——, 1983, Spasmodic tremor and possible magma injection in Long Valley caldera, eastern California: Science, v. 219, p. 1432–1433.

Ryall, A. S., and Savage, W. U., 1969, A comparison of seismological effects for the Nevada underground test Boxcar with natural earthquakes in the Nevada region: Journal of Geophysical Research, v. 74, p. 4281–4289.

Ryall, A. S., and Vetter, U. R., 1982, Seismicity related to geothermal development in Dixie Valley, Nevada: Reno, University of Nevada Final Report on USDOE Contract DE-AC08-79-NV10054, 102 p.

Ryall, A. S., Slemmons, D. B., and Gedney, L. D., 1966, Seismicity, tectonism, and surface faulting in the western United States during historic times: Seismological Society of America Bulletin, v. 156, p. 1105–1135.

Savage, J. C., and Clark, M. M., 1982, Magnetic resurgence in the Long Valley caldera, California: Possible cause of the 1980 Mammoth Lakes earthquakes: Science, v. 217, p. 531–533.

Savage, J. C., and Cockerham, R. S., 1987, Quasi-periodic occurrence of earthquakes in the 1978–1986 Bishop–Mammoth Lakes sequence, eastern California: Seismological Society of America Bulletin, v. 77, p. 1347–1358.

Savage, J. C., and Hastie, L. M., 1969, A dislocation model for the Fairview Peak, Nevada, earthquake: Seismological Society of America Bulletin, v. 59, p. 1937–1948.

Schwartz, D. P., and Coppersmith, K. J., 1984, Fault behavior and characteristic earthquakes; Examples from the Wasatch and San Andreas fault zones: Journal of Geophysical Research, v. 89, p. 5681–5698.

Shawe, D. E., 1965, Strike-slip control of Basin-Range structure indicated by historical faults in western Nevada: Geological Society of America Bulletin, v. 76, p. 1361–1378.

Sipkin, S. A., 1986, Interpretation of non-double-couple earthquake mechanisms derived from moment tensor inversion: Journal of Geophysical Research, v. 91, no. B1, p. 531–547.

Slemmons, D. B., 1957a, Geologic setting for the Fallon-Stillwater earthquakes of 1954: Seismological Society of America Bulletin, v. 47, p. 4–9.

——, 1957b, Geological effects of the Dixie Valley–Fairview Peaks, Nevada, earthquakes of December 16, 1954: Seismological Society America Bulletin, v. 47, p. 353–375.

——, 1967, Pliocene and Quaternary crustal movements of the Basin-and-Range Province, U.S.A.: Osaka City University Journal of Geosciences, v. 10, p. 91–103.

Slemmons, D. B., Steinbrugge, K. V., Tocher, D., Oakeshott, G. B., and Gianella, V. P., 1959, Wonder, Nevada, earthquake of 1903: Seismological Society of America Bulletin, v. 49, p. 251–256.

Slemmons, D. B., Jones, A. E., and Gimlett, J. I., 1965, Catalog of Nevada earthquakes, 1852–1960: Seismological Society of America Bulletin, v. 55, p. 537–583.

Smith, B. E., Hamilton, R. M., and Jackson, W. H., 1971, Seismicity of the central Nevada Test Area, 26 September 1969–1 October 1970: U.S. Geological Survey Report USGS-474-109, 27 p.; available only from U.S. Department of Commerce National Technical Information Service, Springfield, Virginia 22161.

Smith, B. E., Coakley, J. M., and Hamilton, R. M., 1972, Distribution, focal mechanisms, and frequency of earthquakes in the Fairview Peak area, Nevada: Seismological Society of America Bulletin, v. 62, p. 1223–1240.

Smith, K. D., and Priestley, K. F., 1988, The foreshock sequence of the 1986 Chalfont, California, earthquake: Seismological Society of America Bulletin, v. 78, p. 172–187.

Smith, R. B., 1978, Seismicity, crustal structure, and intraplate tectonics of the interior of the western Cordillera, *in* Smith, R. B., and Eaton, G. P., eds., Cenozoic tectonics and regional geophysics of the western Cordillera: Geological Society of America Memoir 152, p. 111–114.

Smith, R. B., and Bruhn, R. L., 1984, Intraplate extensional tectonics of the eastern basin range; Inferences on structural style from seismic reflection data, regional tectonics, and thermal-mechanical models of brittle-ductile deformation: Journal of Geophysical Research, v. 89, p. 5733–5762.

Smith, R. B., and Lindh, A. G., 1978, Fault plane solutions of the western United States; A compilation, *in* Smith, R. B., and Eaton, G. P., eds., Cenozoic tectonics and regional geophysics of the western Cordillera: Geological Society of America Memoir 152, p. 107–109.

Smith, R. B., and Richins, W. D., 1984, Seismicity and earthquake hazards of Utah and the Wasatch Front; Paradigm and paradox, *in* Hays, W. W., and Gori, P. L., eds., Evaluation of regional and urban earthquake hazards and risk in Utah; Proceedings of Conference 26: U.S. Geological Survey Open-File Report 84-763, p. 73–112.

Smith, R. B., Richins, W. D., and Doser, D. I., 1985, The 1983, Borah Peak, Idaho, earthquake; Regional seismicity, kinematics of faulting, and tectonic mechanism, *in* Stein, R. S., and Bucknam, R. C., eds., Proceedings of Workshop 28 on the Borah Peak, Idaho, Earthquake: U.S. Geological Survey Open-File Report 85-290, v. A, p. 236–263.

Snay, R. A., Cline, M. W., and Timmermann, E. L., 1985, Dislocation models for the 1954 earthquake sequence in Nevada: U.S. Geological Survey Open-File Report 85-290, p. 531–555.

Snyder, R. P., 1971, Composite postshot fracture map of Pahute Mesa, Nevada Test Site: U.S. Geological Survey Report USGS-474-100, 17 p.; available only from U.S. Department of Commerce National Technical Information Service, Springfield, Virginia 22161.

——, 1973, Recent fault movement on Pahute Mesa, Nevada Test Site, from May 1970 through June 1973: U.S. Geological Survey Report USGS-474-137, 32 p.; available only from U.S. Department of Commerce National Technical Information Service, Springfield, Virginia 22161.

Sonder, L. J., England, P. C., and Hoseman, G. A., 1986, Continuum calculations of continental deformation in transcurrent environments: Journal of Geophysical Research, v. 91, no. B5, p. 4797–4810.

Spencer, J. E., and Chase, C. G., 1989, Role of crustal flexure in initiation of low-angle normal faults and implications for structural evolution of the Basin and Range Province: Journal of Geophysical Research, v. 94, p. 1765–1775.

Stauder, W., and Ryall, A. S., 1967, Spatial distribution and source mechanism of microearthquakes in central Nevada: Seismological Society of America Bulletin, v. 57, p. 1317–1345.

Steinbrugge, K. V., and Moran, D. F., 1956, Damage caused by the earthquakes of July 6 and August 23, 1954: Seismological Society of America Bulletin, v. 46, p. 15–33.

Stewart, J. H., 1978, Basin-Range structure in western North America; A review, *in* Smith, R. B., and Eaton, G. P., eds., Cenozoic tectonics and regional geophysics of the western Cordillera: Geological Society of America Memoir 152, p. 1–31.

——, 1980, Regional tilt patterns of late Cenozoic Basin-Range fault blocks, western United States: Geological Society of America Bulletin, v. 91, p. 460–464.

——, 1988, Tectonics of the Walker Lane belt, western Great Basin; Mesozoic and Cenozoic deformation in a zone of shear, *in* Ernst, W. G., ed., Metamorphism and cause of evolution of the western United States, Ruby volume 7: Englewood Cliffs, New Jersey, Prentice-Hall, p. 683–713.

Tarr, A. C., and Rogers, A. M., 1986, Analysis of earthquake data recorded by digital field seismic systems, Jackass Flats, Nevada: U.S. Geological Survey Open-File Report 86-420, 67 p.

Thenhaus, P. C., and Barnhard, T. P., 1989, Regional termination and segmentation of Quaternary fault belts in the Great Basin, Nevada and Utah: Seismological Society of America Bulletin, v. 79, p. 1426–1438.

Tocher, D., 1956, Movement on the Rainbow Mountain fault: Seismological Society of America Bulletin, v. 46, p. 10–14.

——, 1957, The Dixie Valley–Fairview Peak earthquakes of December 16, 1954; Introduction: Seismological Society of America Bulletin, v. 47, p. 299–300.

——, 1975, On crustal plates: Seismological Society of America Bulletin, v. 65, p. 1495–1500.

Townley, S. D., and Allen, M. W., 1939, Descriptive catalog of earthquakes of the Pacific coast of the United States 1769 to 1928: Seismological Society of America Bulletin, v. 29, p. 1–297.

VanWormer, J. D., and Ryall, A., 1980, Sierra Nevada–Great Basin boundary zone; Earthquake hazard related to structure, active tectonic processes, and anomalous patterns of earthquake occurrence: Seismological Society of America Bulletin, v. 70, p. 1557–1572.

Vetter, V. R., 1984, Focal mechanisms and crustal stress patterns in western Nevada and eastern California: Annales Geophysicae, v. 2, p. 699–710.

Vetter, V. R., and Ryall, A. S., 1983, Systematic change of focal mechanisms with depth in the western Great Basin: Journal of Geophysical Research, v. 88, p. 8237–8250.

Wallace, R. E., 1978, Patterns of faulting and seismic gaps in the Great Basin Province: U.S. Geological Survey Open-File Report 78-943, p. 857–868.

——, 1984a, Patterns and timing of late Quaternary faulting in the Great Basin Province and relation to some regional tectonic features: Journal of Geophysical Research, v. 89, p. 5763–5769.

——, 1984b, Fault scarps formed during the earthquakes of October 2, 1915, in Pleasant Valley, Nevada, and some tectonic implications in faulting related to the 1915 earthquakes in Pleasant Valley, Nevada: U.S. Geological Survey Professional Paper 1274-A, 33 p.

——, 1987, Grouping and migration of surface faulting and variations in slip rates on faults in the Great Basin Province: Seismological Society of America Bulletin, v. 77, no. 3, p. 868–876.

Wallace, R. E., and Whitney, R. A., 1984, Late Quaternary history of the Stillwater seismic gap, Nevada: Seismological Society of America Bulletin, v. 74, no. 1, p. 301–314.

Wallace, T. C., Helmberger, D. V., and Engen, G. R., 1983, Evidence of tectonic release from underground nuclear explosions in long-period P-waves: Seismological Society of America Bulletin, v. 73, p. 593–613.

——, 1985, Evidence of tectonic release from underground nuclear explosions in long-period S-waves: Seismological Society of America Bulletin, v. 75, p. 157–174.

Wallace, T. C., Helmberger, D. V., and Lay, J., 1986, Reply *to* Comments by A. Douglas, J. B. Yolung, and N. S. Lyman and a note on the revised moments for Pahute Mesa tectonic release: Seismological Society of America Bulletin v. 76, p. 313–318.

Wernicke, B., 1981, Low-angle normal faults in the Basin and Range Province; Nappe tectonics in an extending orogen: Nature, v. 291, p. 645–648.

Wernicke, B., Christiansen, R. L., England, P. C., and Sonder, L. J., 1987, Tectonomagmatic evolution of Cenozoic extension in the North American Cordillera, *in* Coward, M. P., and others, eds., Continental extensional tectonics: Geological Society of London Special Publication 28, p. 203–221.

Wernicke, B., Axen, G. J., and Snow, J. K., 1988, Basin and Range extensional tectonics at the latitude of Las Vegas, Nevada: Geological Society of America Bulletin, v. 100, p. 1738–1757.

Westphal, W. H., and Lange, A. L., 1967, Local seismic monitoring; Fairview Peak area, Nevada: Seismological Society of America Bulletin, v. 57, p. 1279–1298.

Whitten, C. A., 1957, Geodetic measurements in the Dixie Valley area: Seismological Society of America Bulletin, v. 47, p. 321–325.

Wright, L., 1976, Late Cenozoic fault patterns and stress fields in the Great Basin and westward displacement of the Sierra Nevada block: Geology, v. 4, p. 489–414.

Zoback, M. L., 1989, State of stress and modern deformation of the northern Basin and Range Province: Journal of Geophysical Research, v. 94, p. 7105–7128.

Zoback, M. L., and Beanland, S., 1986a, Stress and tectonism along the Walker Lane belt, western Great Basin: EOS Transactions of the America Geophysical Union, v. 67, no. 44, p. 1225.

——, 1986b, Temporal variations in stress magnitude and style of faulting along the Sierran frontal fault system: Geological Society of America Abstracts with Programs, v. 18, p. 801.

Zoback, M. L., and Zoback, M. D., 1980, State of stress in the conterminous United States: Journal of Geophysical Research, v. 85, p. 6113–6156.

Zoback, M. L., Anderson, R. E., and Thompson, G. A., 1981, Cenozoic evolution of the state of stress and style of tectonism of the Basin and Range Province of the western United States: Royal Society of London Philosophical Transactions, series A, v. 300, p. 407–434.

Manuscript Accepted by the Society August 7, 1989

ACKNOWLEDGMENTS

The authors thank the anonymous reviewers for their helpful comments. Detailed reviews and comments were also provided by R. E. Anderson and W. B. Hamilton, whose help is gratefully acknowledged.

Printed in U.S.A.